Production of light isoscalar mesons in *pp* collisions via gluon-gluon fusion

A. Szczurek[1,2] and
I. Babiarz, W. Schäfer
A. Cisek, P. Lebiedowicz, R. Maciula

[1] The Henryk Niewodniczański Institute of Nuclear Physics
Polish Academy of Sciences [2]University of Rzeszów

Krakow, May 10, 2020

Contents

- Introduction
- $pp \to \eta_c$ and $pp \to \chi_{c0}$ (previous studies)
- $pp \to f_0(980)$
  - $\gamma^*\gamma^* \to f_0(980)$
  - Color evaporation model
  - k_t-factorization approach to gluon-gluon fusion
- $pp \to f_2(1270)$
  - $\gamma^*\gamma^* \to f_2(1270)$ and $g^*g^* \to f_2(1270)$ coupling
  - k_t-factorization approach to gluon-gluon fusion
  - Unintegrated gluon distributions
  - $\pi\pi$ final state rescattering
  - Results

Contents

Introduction

- The mechanism of meson production in proton-proton collisions is not fully undersood. The string-model is an option considered e.g. in Phythia. But not all meson production can be explained via string fragmentation.
- The gluon-gluon fusion for η_c and χ_c quarkonium production was shown recently to be the dominant mechanism [1,2].
- In contrast the mechanism of light meson production is not known. Is there gluon-gluon fusion important effect ? Recently we have considered production of $f_0(980)$ (scalar), $f_2(1270)$ (tensor) and shown that gluon-gluon fusion is important contribution but not sufficient to describe ALICE data.
- Very recently we considered production of ϕ and η' mesons. Especially production of η' is very interesting.
- Here we review our recent works.

Our recent paper

[1] I. Babiarz, R. Pasechnik, W. Schäfer and A. Szczurek, JHEP02, 037 (2020).
[2] I. Babiarz, R. Pasechnik, W. Schäfer and A. Szczurek, JHEP06, 101 (2020).
[3] P. Lebiedowicz, R. Maciula and A. Szczurek, Phys. Lett. **B806** 135475 (2020).
[4] P. Lebiedowicz and A. Szczurek, Phys. Lett. **B810** 135816 (2020).
[5] A. Cisek and A. Szczurek, arXiv:2103.08954, accepted in Phys. Rev. **D**.

Introduction

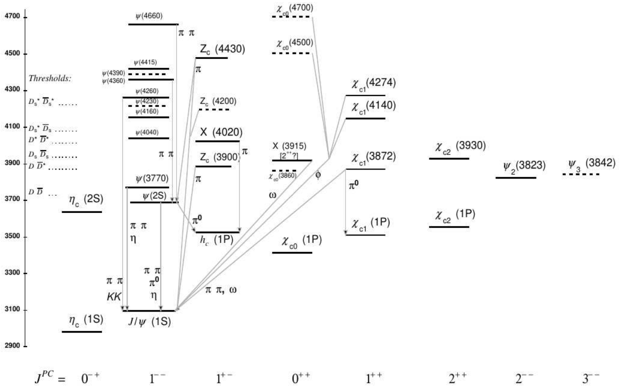

Description of the mechanism $\gamma^*\gamma^* \to \eta_c(1S, 2S)$

Babiarz, Goncalves, Pasechnik, Schäfer and Szczurek,
Phys. Rev. **D100**, 054018 (2019).

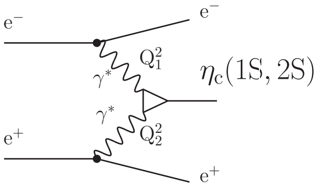

$$\mathcal{M}_{\mu\nu}(\gamma^*(q_1)\gamma^*(q_2) \to \eta_c) = 4\pi\alpha_{\rm em}\,(-i)\varepsilon_{\mu\nu\alpha\beta}q_1^\alpha q_2^\beta\, F(Q_1^2, Q_2^2)$$

Light-front representation of the transition form factor:

$$F(Q_1^2, Q_2^2) = e_c^2\sqrt{N_c}4m_c \cdot \int \frac{dzd^2\mathbf{k}}{z(1-z)16\pi^3}\psi(z,\mathbf{k})$$
$$\left\{\frac{1-z}{(\mathbf{k}-(1-z)\mathbf{q}_2)^2 + z(1-z)\mathbf{q}_1^2 + m_c^2} + \frac{z}{(\mathbf{k}+z\mathbf{q}_2)^2 + z(1-z)\mathbf{q}_1^2 + m_c^2}\right\}.$$

Nonrelativistic quarkonium wave functions

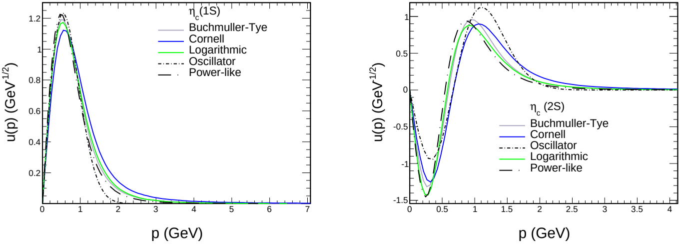

Radial momentum-space wave function for different potentials.

Radial spatial wave function are obtained by solving the Schrödinger equation.

J. Cepila, J. Nemchik, M. Krelina and R. Pasechnik, arXiv:1901.02664 [hep-ph].

$$\frac{\partial^2 u(r)}{\partial r^2} = (V_{\rm eff}(r) - \epsilon)u(r)\,, \qquad u(r) = \sqrt{4\pi}\, r\psi(r)\,,$$

$$\int_0^\infty |u(r)|^2 dr = 1 \quad \Rightarrow \quad \int_0^\infty |u(p)|^2 dp = 1$$

Light-front wave functions

We treat the η_c as a bound state of a charm quark and antiquark, assuming that the dominant contribution comes from the $c\bar{c}$ component in the Fock-state expansion:

$$|\eta_c; P_+, \boldsymbol{P}\rangle = \sum_{i,j,\lambda,\bar{\lambda}} \frac{\delta^i_j}{\sqrt{N_c}} \int \frac{dz d^2\boldsymbol{k}}{z(1-z)16\pi^3} \Psi_{\lambda\bar{\lambda}}(z,\boldsymbol{k}) |c_{i\lambda}(zP_+, \boldsymbol{p}_c) \bar{c}^j_{\bar{\lambda}}((1-z)P_+, \boldsymbol{p}_{\bar{c}})\rangle + \dots \tag{1}$$

Here the c-quark and $\bar{c}$-antiquark carry a fraction z and $1-z$ respectively of the η_c's plus-momentum. The light-front helicites of quark and antiquark are denoted by $\lambda, \bar{\lambda}$, and take values ± 1. The transverse momenta of quark and antiquark are

$$\boldsymbol{p}_c = \boldsymbol{k} + z\boldsymbol{P}\,, \quad \boldsymbol{p}_{\bar{c}} = -\boldsymbol{k} + (1-z)\boldsymbol{P}\,. \tag{2}$$

The light-cone representation is obtained by Terentev's prescription valid for weakly bound systems.

Light-front wave functions

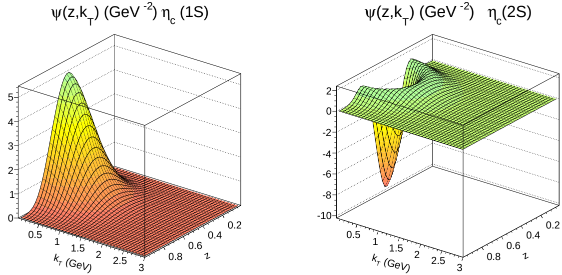

Radial light-front wave function for Buchmüller-Tye potential.

$$\text{Terentev prescription} \Rightarrow \mathbf{p} = \mathbf{k}, \quad p_z = (z - \tfrac{1}{2}) M_{c\bar{c}},$$

$$\psi(z, \mathbf{k}) = \frac{\pi}{\sqrt{2 M_{c\bar{c}}}} \frac{u(p)}{p} \, .$$

Normalized transition form factor $\tilde{F}(Q^2, 0)$

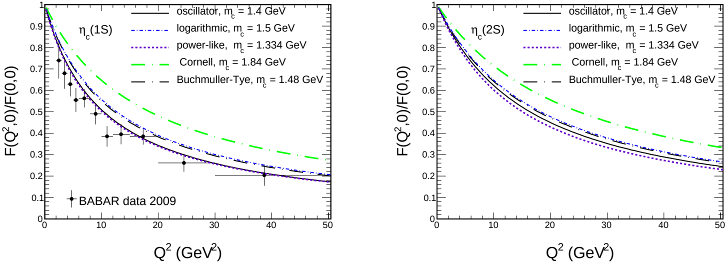

Normalized transition form factor $\tilde{F}(Q^2, 0)$ as a function of photon virtuality Q^2. The BaBar data are shown for comparison.

J. P. Lees *et al.* [BaBar Collaboration], Phys. Rev. D **81**, 052010 (2010) [arXiv:1002.3000 [hep-ex]].

Transition form factor $F(Q_1^2, Q_2^2)$ for $\gamma^*\gamma^* \to \eta_c(1S, 2S)$

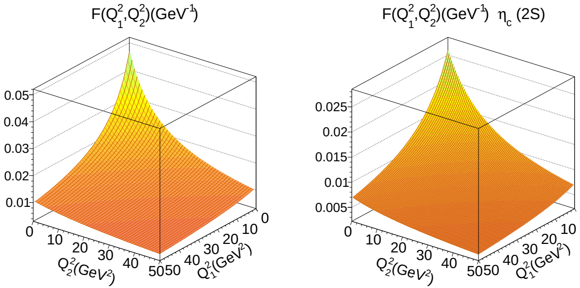

Transition form factor for $\eta_c(1S)$ and $\eta_c(2S)$ for Buchmüller-Tye potential. The $F(Q_1^2, Q_2^2)$ should obey Bose symmetry.

Asymptotic behaviour of $Q^2 F(Q^2, 0)$

The rate of approaching of $Q^2 F(Q^2)$ to its asymptotic value predicted by Brodsky and Lepage

G. P. Lepage and S. J. Brodsky, Phys. Rev. D **22**, 2157 (1980).

$Q^2 F(Q^2) \longrightarrow \frac{8}{3} f_{\eta_c}$, while $Q^2 \longrightarrow \infty$

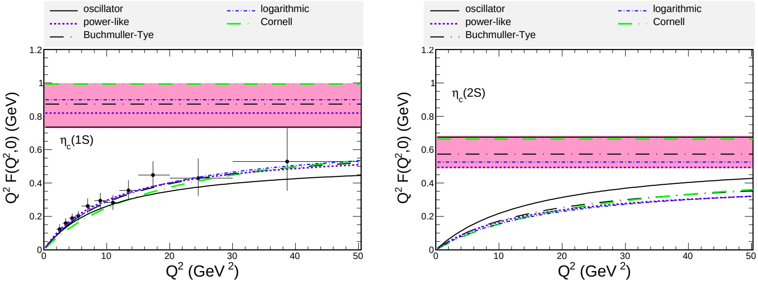

$Q^2 F(Q^2, 0)$ as a function of photon virtuality Q^2. The horizontal lines $\frac{8}{3} f_{\eta_c}$ are shown for reference.

Inclusive production of η_c quarkonia in proton-proton collisions

The diagram below illustrates the situation adequate for the k_T-factorization calculations used in the present paper.

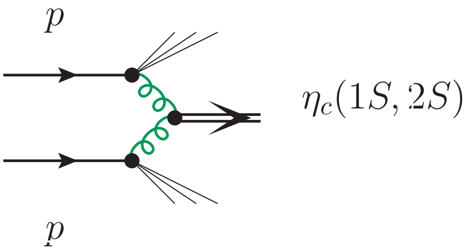

Rysunek: Generic diagram for the inclusive process of η_c(1S) or η_c(2S) production in *pp* scattering via two gluons fusion.

I. Babiarz, R. Pasechnik, W. Schäfer and A. Szczurek, arXiv:1911.03403

k_t-factorization approach

The inclusive cross section for η_c-production via the $2 \to 1$ gluon-gluon fusion mode is obtained from

$$d\sigma = \int \frac{dx_1}{x_1} \int \frac{d^2\boldsymbol{q}_1}{\pi \boldsymbol{q}_1^2} \mathcal{F}(x_1, \boldsymbol{q}_1^2) \int \frac{dx_2}{x_2} \int \frac{d^2\boldsymbol{q}_2}{\pi \boldsymbol{q}_2^2} \mathcal{F}(x_2, \boldsymbol{q}_2^2) \frac{1}{2x_1x_2s} \overline{|\mathcal{M}|}^2 \, d\Phi(2 \to 1). \quad (3)$$

The unintegrated gluon distributions are normalized such, that in the DGLAP-limit

$$\mathcal{F}(x, \boldsymbol{q}^2) = \frac{\partial xg(x, \boldsymbol{q}^2)}{\partial \log \boldsymbol{q}^2} \, . \quad (4)$$

Let us denote the four-momentum of the η_c by P. It can be parametrized as:

$$P = (P_+, P_-, \boldsymbol{P}) = \Big(\frac{m_\perp}{\sqrt{2}} e^y, \frac{m_\perp}{\sqrt{2}} e^{-y}, \boldsymbol{P}\Big) \, , \quad (5)$$

k_t-factorization approach

The phase-space element is

$$d\Phi(2 \to 1) = (2\pi)^4 \delta^{(4)}(q_1 + q_2 - P) \frac{d^4 P}{(2\pi)^3} \delta(P^2 - m^2) \quad (6)$$

The gluon four momenta are written as

$$q_1 = (q_{1+}, 0, \boldsymbol{q}_1), \; q_2 = (0, q_{2-}, \boldsymbol{q}_2), \quad (7)$$

with

$$q_{1+} = x_1 \sqrt{\frac{s}{2}}, \; q_{2-} = x_2 \sqrt{\frac{s}{2}}. \quad (8)$$

We can then calculate the phase-space element as

$$d\Phi(2 \to 1) = 2\pi \delta(q_{1_+} - P_+) \delta(q_{2-} - P_-) \delta^{(2)}(\boldsymbol{q}_1 + \boldsymbol{q}_2 - \boldsymbol{P}) \, dP_+ dP_- d^2\boldsymbol{P} \, \delta(2P_+P_- - \boldsymbol{P}^2 - m^2). \quad (9)$$

This gives

$$\begin{aligned} d\Phi(2 \to 1) &= 2\pi \frac{2}{s} \delta(x_1 - \frac{m_\perp}{\sqrt{s}} e^{y}) \delta(x_2 - \frac{m_\perp}{\sqrt{s}} e^{-y}) \delta^{(2)}(\boldsymbol{q}_1 + \boldsymbol{q}_2 - \boldsymbol{P}) \frac{dP_+}{2P_+} d^2\boldsymbol{P} \\ &= \frac{2\pi}{s} \delta(x_1 - \frac{m_\perp}{\sqrt{s}} e^{y}) \delta(x_2 - \frac{m_\perp}{\sqrt{s}} e^{-y}) \delta^{(2)}(\boldsymbol{q}_1 + \boldsymbol{q}_2 - \boldsymbol{P}) dy d^2\boldsymbol{P}. \quad (10) \end{aligned}$$

k_t-factorization approach

We therefore obtain for the inclusive cross section

$$\frac{d\sigma}{dyd^2\boldsymbol{P}} = \int \frac{d^2\boldsymbol{q}_1}{\pi \boldsymbol{q}_1^2} \mathcal{F}(x_1, \boldsymbol{q}_1^2) \int \frac{d^2\boldsymbol{q}_2}{\pi \boldsymbol{q}_2^2} \mathcal{F}(x_2, \boldsymbol{q}_2^2)\, \delta^{(2)}(\boldsymbol{q}_1 + \boldsymbol{q}_2 - \boldsymbol{P})\, \frac{\pi}{(x_1 x_2 s)^2} \overline{|\mathcal{M}|^2}, \tag{11}$$

where the momentum fractions $x_{1,2}$ of gluons are

$$x_1 = \frac{m_\perp}{\sqrt{s}} e^y \,,\; x_2 = \frac{m_\perp}{\sqrt{s}} e^{-y}. \tag{12}$$

The off-shell color singlet matrix element is written in terms of the Feynman amplitude as (we restore the color-indices):

$$\mathcal{M}^{ab} = \frac{q_{1\perp}^\mu q_{2\perp}^\nu}{|\boldsymbol{q}_1||\boldsymbol{q}_2|} \mathcal{M}_{\mu\nu}^{ab} = \frac{q_{1+} q_{2-}}{|\boldsymbol{q}_1||\boldsymbol{q}_2|} n_\mu^+ n_\nu^- \mathcal{M}_{\mu\nu}^{ab} = \frac{x_1 x_2 s}{2|\boldsymbol{q}_1||\boldsymbol{q}_2|} n_\mu^+ n_\nu^- \mathcal{M}_{\mu\nu}^{ab} \,. \tag{13}$$

Then, we obtain for the cross section

$$\frac{d\sigma}{dyd^2\boldsymbol{P}} = \int \frac{d^2\boldsymbol{q}_1}{\pi \boldsymbol{q}_1^4} \mathcal{F}(x_1, \boldsymbol{q}_1^2) \int \frac{d^2\boldsymbol{q}_2}{\pi \boldsymbol{q}_2^4} \mathcal{F}(x_2, \boldsymbol{q}_2^2)\, \delta^{(2)}(\boldsymbol{q}_1 + \boldsymbol{q}_2 - \boldsymbol{P})\, \frac{\pi}{4} \overline{|n_\mu^+ n_\mu^- \mathcal{M}_{\mu\nu}|^2}, \tag{14}$$

k_t-factorization approach

The CS matrix element squared averaged over color is

$$\overline{|n_\mu^+ n_\mu^- \mathcal{M}_{\mu\nu}|}^2 = \frac{1}{(N_c^2-1)^2} \sum_{a,b} |n_\mu^+ n_\mu^- \mathcal{M}_{\mu\nu}^{ab}| \, . \tag{15}$$

The matrix element has the form

$$\begin{aligned} n_\mu^+ n_\mu^- \mathcal{M}_{\mu\nu}^{ab} &= 4\pi\alpha_S(-i)[\boldsymbol{q}_1, \boldsymbol{q}_2] \frac{[t^a t^b]}{\sqrt{N_c}} \, I(\boldsymbol{q}_1^2, \boldsymbol{q}_2^2) \\ &= 4\pi\alpha_S(-i)\frac{1}{2}\delta^{ab} \frac{1}{\sqrt{N_c}} [\boldsymbol{q}_1, \boldsymbol{q}_2] \, I(\boldsymbol{q}_1^2, \boldsymbol{q}_2^2) \end{aligned} \tag{16}$$

It is related to the $\gamma^*\gamma^*\eta_c$ transition formfactor through the relation

$$F(Q_1^2, Q_2^2) = e_c^2 \sqrt{N_c} \, I(\boldsymbol{q}_1^2, \boldsymbol{q}_2^2) \, . \tag{17}$$

The vector product $[\boldsymbol{q}_1, \boldsymbol{q}_2]$ is defined as

$$[\boldsymbol{q}_1, \boldsymbol{q}_2] = q_1^x q_2^y - q_1^y q_2^x = |\boldsymbol{q}_1||\boldsymbol{q}_2| \sin(\phi_1 - \phi_2) \, . \tag{18}$$

k_t-factorization approach

Then, the averaged matrix element squared becomes

$$\overline{|n_\mu^+ n_\mu^- \mathcal{M}_{\mu\nu}|}^2 = 16\pi^2 \alpha_S^2 \frac{1}{4}\frac{1}{N_c} |[\boldsymbol{q}_1, \boldsymbol{q}_2]\, I(\boldsymbol{q}_1^2, \boldsymbol{q}_2^2)|^2 \frac{1}{(N_c^2-1)^2} \sum_{a,b} \delta^{ab}\delta^{ab}$$

$$= 4\pi^2 \alpha_S^2 \frac{1}{N_c(N_c^2-1)} |[\boldsymbol{q}_1, \boldsymbol{q}_2]\, I(\boldsymbol{q}_1^2, \boldsymbol{q}_2^2)|^2 \qquad (19)$$

This leads to our final result:

$$\frac{d\sigma}{dy d^2\boldsymbol{P}} = \int \frac{d^2\boldsymbol{q}_1}{\pi \boldsymbol{q}_1^4} \mathcal{F}(x_1, \boldsymbol{q}_1^2) \int \frac{d^2\boldsymbol{q}_2}{\pi \boldsymbol{q}_2^4} \mathcal{F}(x_2, \boldsymbol{q}_2^2)\, \delta^{(2)}(\boldsymbol{q}_1 + \boldsymbol{q}_2 - \boldsymbol{P}) \frac{\pi^3 \alpha_S^2}{N_c(N_c^2-1)} |[\boldsymbol{q}_1, \boldsymbol{q}_2]\, I(\boldsymbol{q}_1^2, \boldsymbol{q}_2^2)|^2 .$$

In real calculation we take $\mu_F^2 = m_T^2$ and for renormalization scale(s)

$$\alpha_s^2 \to \alpha_s(max(m_t^2, q_{t,1}^2))\alpha_s(max(m_t^2, q_{t,2}^2)) \,. \qquad (20)$$

Normalization of the $g^*g^*\eta_c(1S, 2S)$ form factors

From the proportionality of the $g^*g^*\eta_c$ and $\gamma^*\gamma^*\eta_c$ vertices to the leading order (LO), we obtain, that at LO:

$$\Gamma_{\rm LO}(\eta_c \to gg) = \frac{N_c^2 - 1}{4N_c^2} \frac{1}{e_c^4} \left(\frac{\alpha_s}{\alpha_{\rm em}}\right)^2 \Gamma_{\rm LO}(\eta_c \to \gamma\gamma)\,, \tag{21}$$

where the LO $\gamma\gamma$ width is related to the transition form factor for vanishing virtualities through

$$\Gamma_{\rm LO}(\eta_c \to \gamma\gamma) = \frac{\pi}{4}\alpha_{\rm em}^2 M_{\eta_c}^3 |F(0,0)|^2\,. \tag{22}$$

At NLO, the expressions for the widths read (see Lansberg et al.)

$$\begin{aligned} \Gamma(\eta_c \to \gamma\gamma) &= \Gamma_{\rm LO}(\eta_c \to \gamma\gamma) \left(1 - \frac{20-\pi^2}{3}\frac{\alpha_s}{\pi}\right), \\ \Gamma(\eta_c \to gg) &= \Gamma_{\rm LO}(\eta_c \to gg) \left(1 + 4.8\,\frac{\alpha_s}{\pi}\right). \end{aligned} \tag{23}$$

Unintegrated gluon distributions

We use a few different UGDs which are available from the literature, e.g. from the TMDLib package (Hautmann et al.) or the CASCADE code (Jung et al.).

1. Firstly we use a glue constructed according to the prescription initiated in (Kimber et al.) and later updated in (Martin et al.), which we label below as "KMR". It uses as an input the collinear gluon distribution from Harland-Lang et al.
2. Secondly, we employ two UGDs obtained by Kutak. There are two versions of this UGD. Both introduce a hard scale dependence via a Sudakov form factor into solutions of a small-x evolution equation. The first version uses the solution of a linear, BFKL evolution with a resummation of subleading terms and is denoted by "Kutak (linear)". The second UGD, denoted as "Kutak (nonlinear)" uses instead a nonlinear evolution equation of Balitsky-Kovchegov type. Both of the Kutak's UGDs can be applied only in the small-x regime, $x < 0.01$.
3. The third type of UGD has been obtained by Hautmann and Jung from a description of precise HERA data on deep inelastic structure function by a solution of the CCFM evolution equations. We use "Set 2".

KMR UGDF

For the case of the KMR UGD, it has recently been shown (Maciula, Szczurek), that it includes effectively higher order corrections of the collinear factorization approach. In this sense should give, within our approach, a result similar to that found recently in the NLO approach (Feng, Lansberg et al.) at not too small transverse momenta.

In our approach we can go to very small transverse momenta close to $p_T = 0$.

Results for the LHC

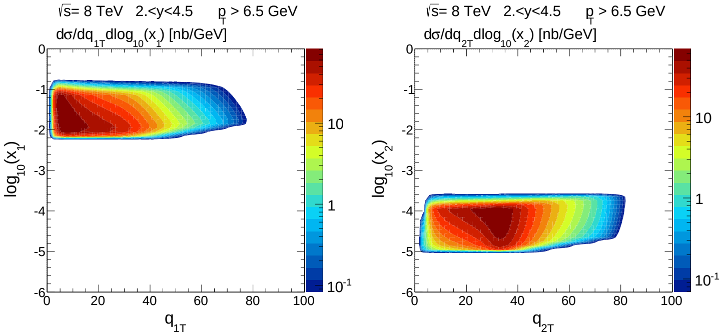

Rysunek: Two-dimensional distributions in (x_1, q_{1T}) (left panel) and in (x_2, q_{2T}) (right panel) for $\eta_c(1S)$ production for $\sqrt{s} = 8$ TeV. In this calculation the KMR UGD was used for illustration.

Results for the LHC

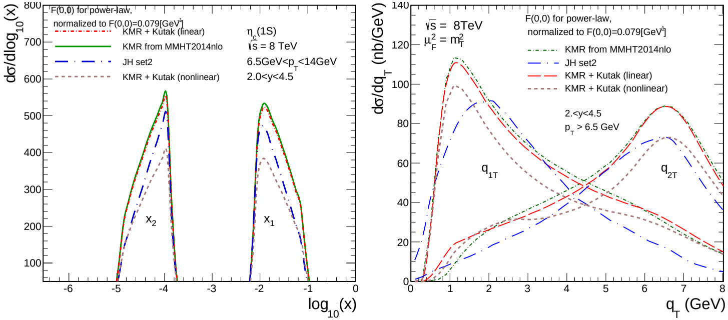

Rysunek: Distributions in $\log_{10}(x_1)$ or $\log_{10}(x_2)$ (left panel) and distributions in q_{1T} or q_{2T} (right panel) for the LHCb kinematics. Here the different UGDs were used in our calculations. Here we show an example for $\sqrt{s} = 8$ TeV.

Results for the LHC

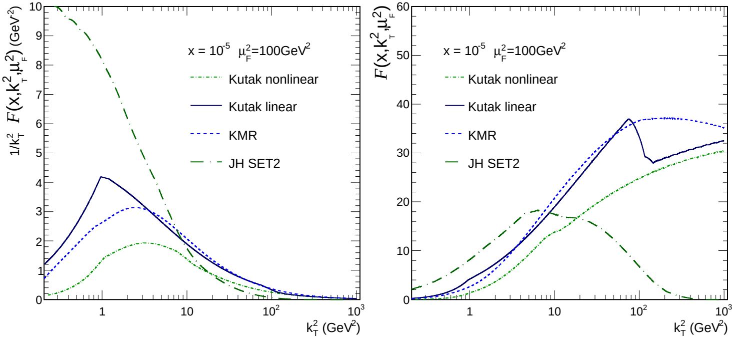

Rysunek: Unintegrated gluon densities for typical scale $\mu^2 = 100$ GeV^2 for $\eta_c(1S)$ production in proton-proton scattering at LHCb kinematics.

UGDs are quite different but ...

Results for the LHC

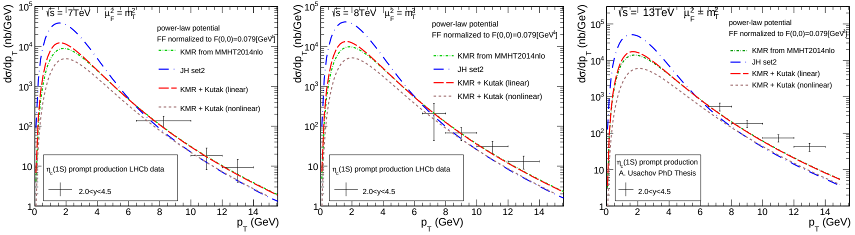

Rysunek: Differential cross section as a function of transverse momentum for prompt $\eta_c(1S)$ production compared with the LHCb data (Aaij et al.) for $\sqrt{s} = 7, 8\,\mathrm{TeV}$ and preliminary experimental data (Usachov PhD) for $\sqrt{s}$ = 13 TeV. Different UGDs were used. Here we used the $g^*g^* \to \eta_c(1S)$ form factor calculated from the power-law potential.

$F(0,0)$ extracted from $\Gamma_{\eta_c(1S)}$ at NLO accuracy

Results for the LHC, $\eta_c(2S)$

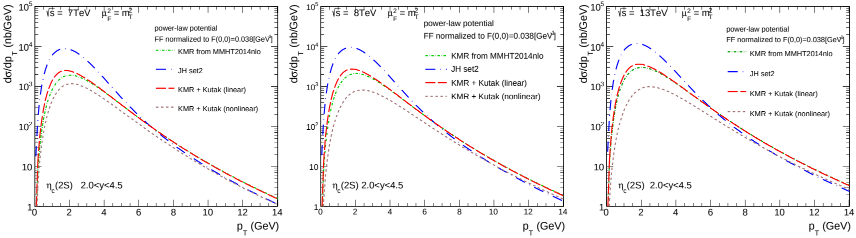

Rysunek: Differential cross section as a function of transverse momentum for prompt $\eta_c(2S)$ production for $\sqrt{s} = 7, 8, 13\,\mathrm{TeV}$.

$F(0,0)$ extracted from $\Gamma_{\eta_c(2S)}$ at NLO accuracy

Results for the LHC, different form factors

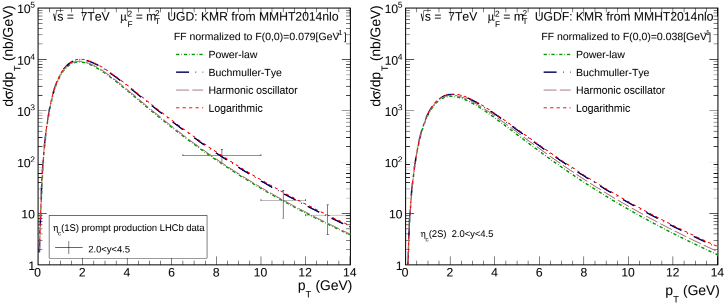

Rysunek: Transverse momentum distributions calculated with different form factors obtained from different potential models of quarkonium wave function and one common normalization of $|F(0,0)|$.

Results for the LHC

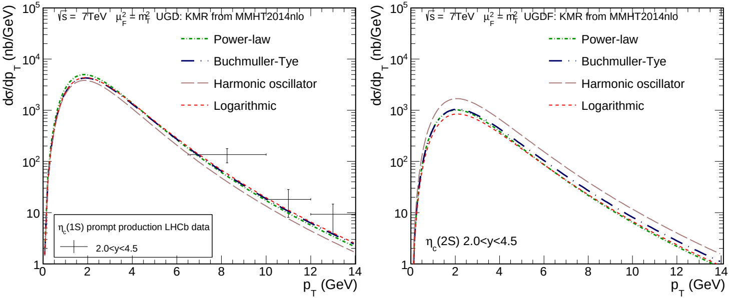

Rysunek: Distributions calculated with several different form factors obtained from different potential models of quarkonium.

Different F(0,0).

Results for the LHC, integrated cross section

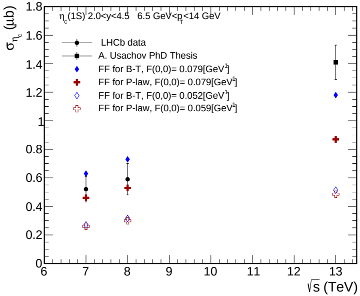

Rysunek: The integrated cross section computed within LHCb range of p_T and y with our transition form factors, compared to experimental values. Here red crosses represent values for Buchmüller-Tye potential (B-T) and deltoids for Power-law potential (P-law).

Somewhat faster grow for experimental data.

Results for the LHC, effect of form factor

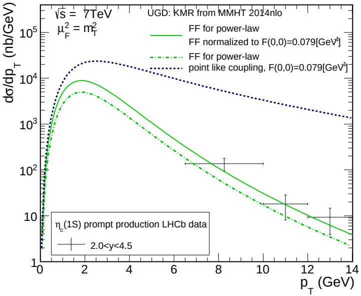

Rysunek: Comparison of results for two different transition form factor, computed with the KMR unintegrated gluon distribution. We also show result when the (q_{1T}^2, q_{2T}^2) dependence of the transition form factor is neglected.

Is the form factor included in collinear calculations ?

Not always.

Results for the ATLAS/CMS kinematics

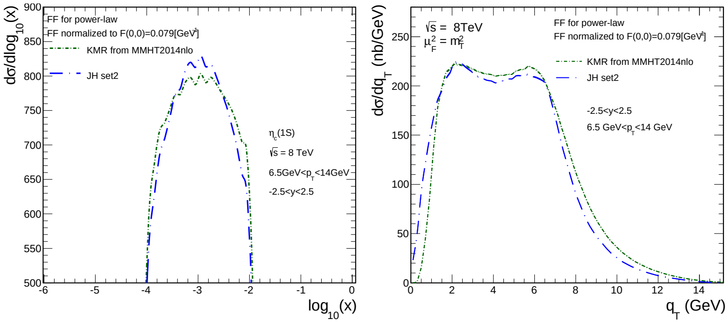

Rysunek: Distribution in $\log_{10}(x_1)$ or $\log_{10}(x_2)$ (left panel) and distribution in q_{1T} or q_{2T} (right panel) for ATLAS or CMS conditions.

Not so small x_1, x_2 as for LHCb.

Results for the ATLAS/CMS kinematics

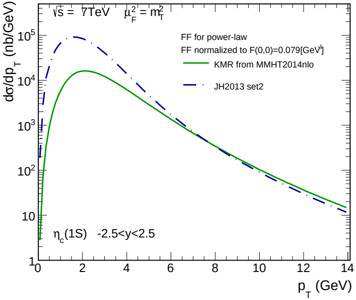

Rysunek: Transverse momentum distribution of prompt $\eta_c(1S)$ for $-2.5 < y < 2.5$ and $\sqrt{s} = 7$ TeV.

$f_0(980)$ production in $\gamma^*\gamma^*$ fusion

In the formalism presented by in Pascalutsa et al. the covariant matrix element for the $\gamma^*\gamma^* \to f_0(980)$ process is written as:

$$\mathcal{M}^{\mu\nu} = 4\pi\alpha_{\rm em}\,\frac{\nu}{m_{f_0}}\left[-R^{\mu\nu}(q_1,q_2)\,F_{TT}(Q_1^2,Q_2^2) + \frac{\nu}{X}\left(q_1^\mu + \frac{Q_1^2}{\nu}q_2^\mu\right)\left(q_2^\nu + \frac{Q_2^2}{\nu}q_1^\nu\right)F_{LL}(Q_1^2,Q_2^2)\right], \tag{24}$$

where $\nu = (q_1 \cdot q_2)$, $X = \nu^2 - q_1^2 q_2^2$, and

$$R^{\mu\nu}(q_1,q_2) = -g^{\mu\nu} + \frac{1}{X}\left[\nu\left(q_1^\mu q_2^\nu + q_2^\mu q_1^\nu\right) - q_1^2 q_2^\mu q_2^\nu - q_2^2 q_1^\mu q_1^\nu\right]. \tag{25}$$

Here q_1 and q_2 denote the momenta of the photons, $Q_1^2 = -q_1^2$, $Q_2^2 = -q_2^2$, and m_{f_0} is mass of the $f_0(980)$ meson. In Eq. (83), the scalar meson structure information in encoded in the form factors F_{TT} and F_{LL} which are functions of the virtualities of both photons. F_{TT} or F_{LL} correspond to the situation where either both photons are transverse or longitudinal, respectively. By definition the form factors are dimensionless.

$f_0(980)$ production in $\gamma^*\gamma^*$ fusion

The two-photon decay width of the $f_0(980)$ meson can be calculated as:

$$\Gamma(f_0(980) \to \gamma\gamma) = \frac{\pi\alpha_{\rm em}^2}{4} m_{f_0} |F_{TT}(0,0)|^2 \,. \qquad (26)$$

Only F_{TT} form factor can be constraint from (26). The radiative decay width is relatively well known. Using the average decay width

$$\Gamma(f_0(980) \to \gamma\gamma) = 0.31 \ {\rm keV} \,. \qquad (27)$$

and $m_{f_0} = 980$ MeV we obtain from (26) $|F_{TT}(0,0)| = 0.087$. Then the transverse form factor is parametrized as:

$$\frac{F_{TT}(Q_1^2,Q_2^2)}{F_{TT}(0,0)} = \left(\frac{\Lambda_M^2}{Q_1^2+Q_2^2+\Lambda_M^2}\right) , \qquad (28)$$

$$\frac{F_{TT}(Q_1^2,Q_2^2)}{F_{TT}(0,0)} = \left(\frac{\Lambda_D^2}{Q_1^2+Q_2^2+\Lambda_D^2}\right)^2 , \qquad (29)$$

where cut-off parameters Λ_M or Λ_D are expected to be of order of 1 GeV. Both monopole (98) and dipole (59)

$f_0(980)$ production in $\gamma^*\gamma^*$ fusion

The F_{LL} form factor is rather unknown but via construction do not enter the formula for the radiative decay width (26) as

$$F_{LL}(0, Q_2^2) = F_{LL}(Q_1^2, 0) = 0\,. \tag{30}$$

We propose to use the following parametrization for the F_{LL} form factor:

$$F_{LL}(Q_1^2, Q_2^2) = R_{LL/TT}\,\frac{Q_1^2}{M_0^2 + Q_1^2}\,\frac{Q_2^2}{M_0^2 + Q_2^2}\,F_{TT}(Q_1^2, Q_2^2)\,. \tag{31}$$

Such a form is consistent with a microscopic calculation for $\gamma^*\gamma^* \to \chi_{c0}$ (Babiarz et al.) using quarkonium wave functions obtained from the potential models. In our present case we expect $R_{LL/TT} \approx \pm 0.5$ and $M_0 \sim m_{f_0}$.

Color singlet $g^*g^* \to f_0(980)$ fusion

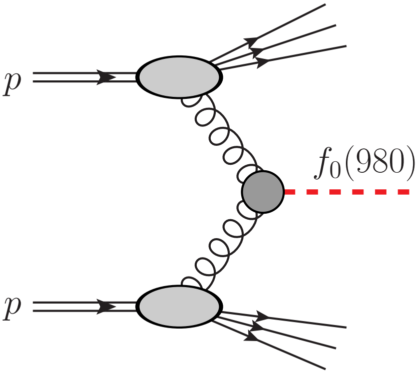

Rysunek: General diagram for inclusive $f_0(980)$ production via gluon-gluon fusion in proton-proton collisions.

Color singlet $g^* g^* \to f_0(980)$ fusion

The differential cross section for inclusive $f_0(980)$ meson production via the $g^* g^* \to f_0(980)$ fusion in the k_t-factorization approach can be written as:

$$\frac{d\sigma}{dy d^2\boldsymbol{p}} = \int \frac{d^2\boldsymbol{q}_1}{\pi \boldsymbol{q}_1^2} \mathcal{F}(x_1, \boldsymbol{q}_1^2) \int \frac{d^2\boldsymbol{q}_2}{\pi \boldsymbol{q}_2^2} \mathcal{F}(x_2, \boldsymbol{q}_2^2)\, \delta^{(2)}(\boldsymbol{q}_1 + \boldsymbol{q}_2 - \boldsymbol{p})\, \frac{\pi}{(x_1 x_2 s)^2} \overline{|\mathcal{M}|^2}\,. \quad (32)$$

Here $\boldsymbol{q}_1$, $\boldsymbol{q}_2$ and $\boldsymbol{p}$ denote the transverse momenta of the gluons and the $f_0(980)$ meson. $\mathcal{M}_{g^* g^* \to f_0}$ is the off-shell matrix element for the hard subprocess and $\mathcal{F}_g$ are the gluon unintegrated distribution functions (UGDFs) for both colliding protons. The UGDFs depend on gluon longitudinal momentum fractions $x_{1,2} = m_T \exp(\pm \mathrm{y})/\sqrt{s}$ and $\boldsymbol{q}_1^2, \boldsymbol{q}_2^2$ entering the hard process.

Color singlet $g^* g^* \to f_0(980)$ fusion

The off-shell matrix element can be written as (we restore the color indices a and b)

$$\mathcal{M}^{ab} = \frac{q_{1t}^{\mu} q_{2t}^{\nu}}{|\boldsymbol{q}_1||\boldsymbol{q}_2|} \mathcal{M}_{\mu\nu}^{ab} = \frac{q_{1+} q_{2-}}{|\boldsymbol{q}_1||\boldsymbol{q}_2|} n^{+\mu} n^{-\nu} \mathcal{M}_{\mu\nu}^{ab} = \frac{x_1 x_2 s}{2|\boldsymbol{q}_1||\boldsymbol{q}_2|} n^{+\mu} n^{-\nu} \mathcal{M}_{\mu\nu}^{ab} \tag{33}$$

with the lightcone components of gluon momenta $q_{1+} = x_1\sqrt{s/2}$, $q_{2-} = x_2\sqrt{s/2}$.
The $g^* g^* \to f_0(980)$ coupling entering in the matrix element squared can be obtained from that for $\gamma^*\gamma^* \to f_0(980)$ coupling by the following replacement:

$$\alpha_{\rm em}^2 \to \alpha_{\rm s}^2 \frac{1}{4N_c(N_c^2-1)} \frac{1}{(< e_q^2 >)^2} \,. \tag{34}$$

Color singlet $g^*g^* \rightarrow f_0(980)$ fusion

$(< e_q^2 >)$ above strongly depends on the flavour structure of the wave function. In the following we consider a few examples of quark-flavour composition:

- $$f_0(980)\rangle = \frac{1}{\sqrt{2}} \left(u\bar{u}\rangle + d\bar{d}\rangle \right) , \qquad (35)$$
- $$f_0(980)\rangle = s\bar{s}\rangle , \qquad (36)$$
- $$f_0(980)\rangle = \frac{1}{\sqrt{2}} \left([su][\bar{s}\bar{u}]\rangle + [sd][\bar{s}\bar{d}]\rangle \right) . \qquad (37)$$

Color singlet $g^* g^* \to f_0(980)$ fusion

In realistic calculations the running of strong coupling constants must be included. In our numerical calculations presented below, we set the factorization scale to $\mu_F^2 = m_T^2$, and the renormalization scale is taken in the form:

$$\alpha_s^2 \to \alpha_s(\max\{m_T^2, \boldsymbol{q}_1^2\})\, \alpha_s(\max\{m_T^2, \boldsymbol{q}_2^2\})\,. \qquad (38)$$

Color evaporation model

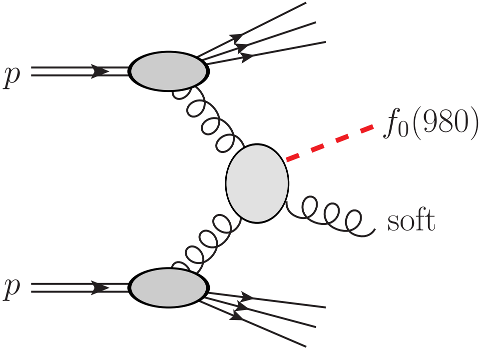

Rysunek: General diagram for inclusive $f_0(980)$ production in proton-proton collisions in the color evaporation approach.

Color evaporation

$$\frac{d\sigma_{f_0}(p_{f_0})}{d^3p_{f_0}} = \mathrm{P_{CEM}} \int_{m_{f_0}-\Delta M}^{m_{f_0}+\Delta M} d^3P_{q\bar{q}}\; dM_{q\bar{q}} \frac{d\sigma_{q\bar{q}}(M_{q\bar{q}}, P_{q\bar{q}})}{dM_{q\bar{q}}\; d^3P_{q\bar{q}}} \delta^3(\vec{p}_{f_0} - \frac{m_{f_0}}{M_{q\bar{q}}}\vec{P}_{q\bar{q}})\,, \quad (39)$$

where $\mathrm{P_{CEM}}$ is the probability of the $q\bar{q} \to f_0(980)$ transition which is fitted to the experimental data, $M_{q\bar{q}}$ and $P_{q\bar{q}} = |\vec{P}_{q\bar{q}}|$ are the invariant mass and momentum of the $q\bar{q}$ system. Here we take $\Delta M = 100$ MeV.

Color evaporation

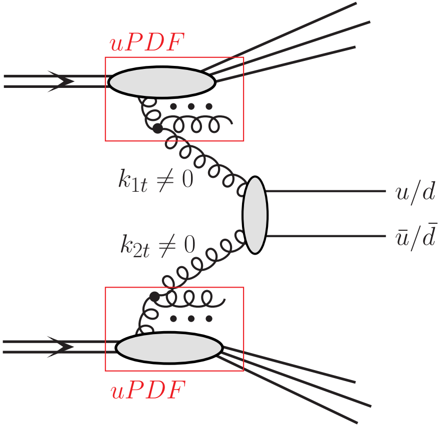

Rysunek: Typical k_t-factorization process with the production of $u\bar{u}$ and $d\bar{d}$ pairs that are intermediate state for color evaporation.

Color evaporation

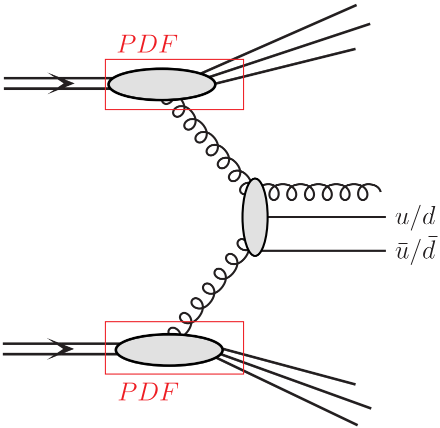

Rysunek: An alternative collinear approach with the production of $u\bar{u}$ and $d\bar{d}$ pairs associated with soft gluon emission that are intermediate state for color evaporation.

Numerical results

To convert to the number of $f_0(980)$ mesons per event, as was presented in Lee (PhD thesis), we use the following relation:

$$\frac{dN}{dp_t} = \frac{1}{\sigma_{\rm inel}} \frac{d\sigma}{dp_t} \,. \quad (40)$$

The inelastic cross section for $\sqrt{s} = 7$ TeV was measured at the LHC and is:

$$\sigma_{\rm inel} = 73.15 \pm 1.26\,({\rm syst.})\,{\rm mb}\,, \quad (41)$$

$$\sigma_{\rm inel} = 71.34 \pm 0.36\,({\rm stat.}) \pm 0.83\,({\rm syst.})\,{\rm mb}\,, \quad (42)$$

as obtained by the TOTEM and ATLAS collaborations, respectively. In our calculations we take $\sigma_{\rm inel} = 72.5$ mb.

Numerical results

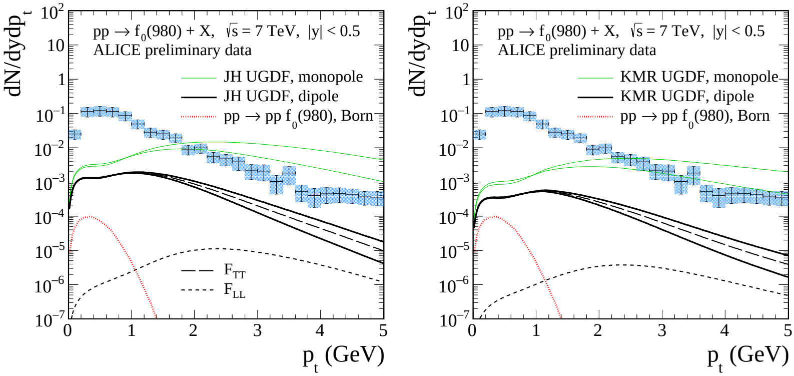

Rysunek: The $f_0(980)$ meson transverse momentum distributions at $\sqrt{s} = 7$ TeV and $|y| < 0.5$. The preliminary ALICE data from [?] are shown for comparison. For the $g^*g^* \to f_0(980)$ contribution two different UGDFs are used: the JH (left panel) and KMR (right panel). Here, the $s\bar{s}$ flavour wave function of $f_0(980)$ is taken into account. Shown are TT and LL components in the amplitude and

Results, color evaporation

In the present study the cross sections for $u\bar{u}$ and $d\bar{d}$ or alternatively $s\bar{s}$ minijet pair production are calculated in the k_t-factorization approach or in the collinear approach. In both cases the calculations are done with the help of the KaTie Monte Carlo code (van Hameren). Considering production of (soft) minijets a real problem is a regularization of the cross section at small transverse momenta. Here we follow the methods adopted for collinear approach in PYTHIA and multiply the calculated cross section by a somewhat arbitrary suppression factor:

$$F_{\rm sup}(p_t) = \frac{p_t^4}{((p_t^0)^2 + p_t^2)^2}\,, \tag{43}$$

where p_t^0 is a free parameter of the model. In the following calculations we take different values of p_t^0, in order to show sensitivity of the results to the choice of this parameter. The parameter goes also into the argument of the strong coupling

Results, color evaporation

Technically, in the numerical calculations here, the suppression factor includes the fact that the transverse momenta of outgoing minijets are not balanced and it takes the following form:

$$F_{\rm sup}^{(2)}(p_{1t}^2, p_{2t}^2) = \frac{p_{1t}^2}{(p_t^0)^2 + p_{1t}^2} \times \frac{p_{2t}^2}{(p_t^0)^2 + p_{2t}^2} \,. \quad (44)$$

The KaTie Monte Carlo generator does not have any problems with the generation of the events in the case of the $2 \to 2$ processes, even if there is no additional cut-off on the outgoing minijets transverse momenta (thus low-p_t cuts are not necessary here). The generated events for massless quarks/antiquarks are weighted by the suppression factor (44).

Results, color evaporation, k_t-factorization

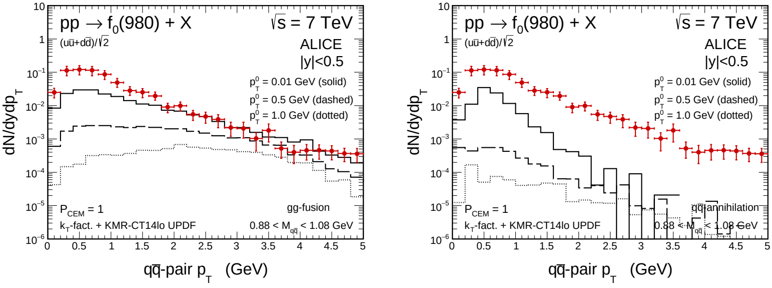

Rysunek: The transverse momentum distribution of $f_0(980)$ for the KMR-CT14lo UPDFs for different p_t^0 in (44) for the gg-fusion (left) and $q\bar{q}$ (right) mechanisms. The calculations were done for $M_{q\bar{q}} \in (0.88, 1.08)$ GeV.

Results, color evaporation, k_t-factorization

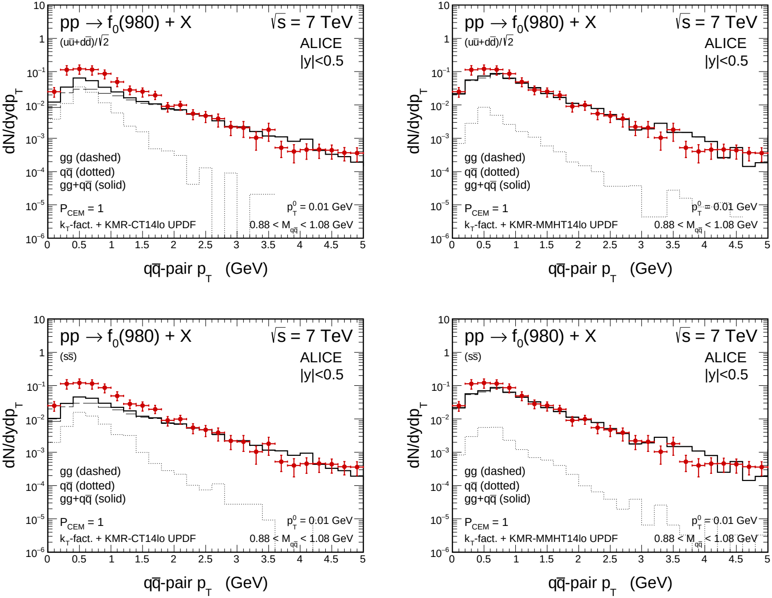

Results, color evaporation model, k_t-factorization

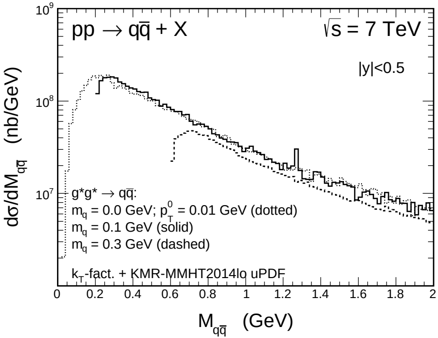

Rysunek: $M_{q\bar{q}}$ invariant mass distribution for three different quark/antiquark masses specified in the figure.

Results, color evaporation, k_t-factorization

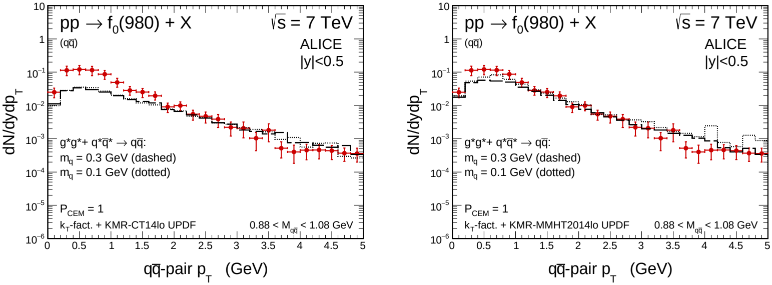

Rysunek: The transverse momentum distributions of $f_0(980)$ for the KMR UPDFs for two masses of produced quark/antiquark: $m_q = 0.1$ GeV (dotted) and $m_q = 0.3$ GeV (dashed). Calculations were done in the $q\bar{q}$ invariant mass region $M_{q\bar{q}} \in (0.88, 1.08)$ GeV.

$2 \to 3$ partonic processes

In the calculations we take into account the $2 \to 3$ partonic processes at the tree-level. So here the $q\bar{q}$-pair is associated with extra gluon or quark which comes from the hard matrix elements. Here we include all the partonic subprocesses with gg-, qg- and $q\bar{q}$-types of initial states. The full list included is:

- gg-fusion:
  $gg \to gu\bar{u}$, $gg \to gd\bar{d}$
- qg-interaction:
  $gu \to uu\bar{u}$, $gd \to du\bar{u}$, $gs \to su\bar{u}$, $g\bar{u} \to \bar{u}u\bar{u}$, $g\bar{d} \to \bar{d}u\bar{u}$, $g\bar{s} \to \bar{s}u\bar{u}$,
  $ug \to uu\bar{u}$, $dg \to du\bar{u}$, $sg \to su\bar{u}$, $\bar{u}g \to \bar{u}u\bar{u}$, $\bar{d}g \to \bar{d}u\bar{u}$, $\bar{s}g \to \bar{s}u\bar{u}$,
  $gu \to ud\bar{d}$, $gd \to dd\bar{d}$, $gs \to sd\bar{d}$, $g\bar{u} \to \bar{u}d\bar{d}$, $g\bar{d} \to \bar{d}d\bar{d}$, $g\bar{s} \to \bar{s}d\bar{d}$,
  $ug \to ud\bar{d}$, $dg \to dd\bar{d}$, $sg \to sd\bar{d}$, $\bar{u}g \to \bar{u}d\bar{d}$, $\bar{d}g \to \bar{d}d\bar{d}$, $\bar{s}g \to \bar{s}d\bar{d}$
- $q\bar{q}$-annihilation:
  $u\bar{u} \to gu\bar{u}$, $d\bar{d} \to gu\bar{u}$, $s\bar{s} \to gu\bar{u}$, $\bar{u}u \to gu\bar{u}$, $\bar{d}d \to gu\bar{u}$, $\bar{s}s \to gu\bar{u}$,
  $d\bar{d} \to gd\bar{d}$, $u\bar{u} \to gd\bar{d}$, $s\bar{s} \to gd\bar{d}$, $\bar{d}d \to gd\bar{d}$, $\bar{u}u \to gd\bar{d}$, $\bar{s}s \to gd\bar{d}$

In the case of the collinear calculations of the $2 \to 3$ processes the suppression factor takes the following form:

$$F^{(3)}_{\rm sup}(p^2_{1t}, p^2_{2t}, p^2_{3t}) = \frac{p^2_{1t}}{(p^0_t)^2 + p^2_{1t}} \times \frac{p^2_{2t}}{(p^0_t)^2 + p^2_{2t}} \times \frac{p^2_{3t}}{(p^0_t)^2 + p^2_{3t}} . \quad (45)$$

Collinear approach, 2 $\longrightarrow$ 3 partonic processes

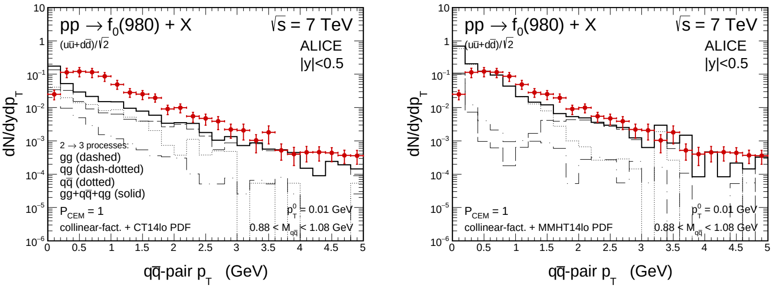

Rysunek: The $f_0(980)$ meson transverse momentum distributions at $\sqrt{s} = 7$ TeV and $|\mathrm{y}| < 0.5$, calculated in the color evaporation model based on the collinear approach, using the CT14lo (left) and MMHT2014lo (right) PDFs together with the preliminary ALICE data (Lee thesis). The calculations were done in quark-antiquark invariant mass region $M_{q\bar{q}} \in (0.88, 1.08)$ GeV. Here the gg, qg and $q\bar{q}$ induced interaction mechanisms are shown separately. Shown are results for the light $q\bar{q}$ scenario (35) for the flavour wave

Introduction to f_2 production

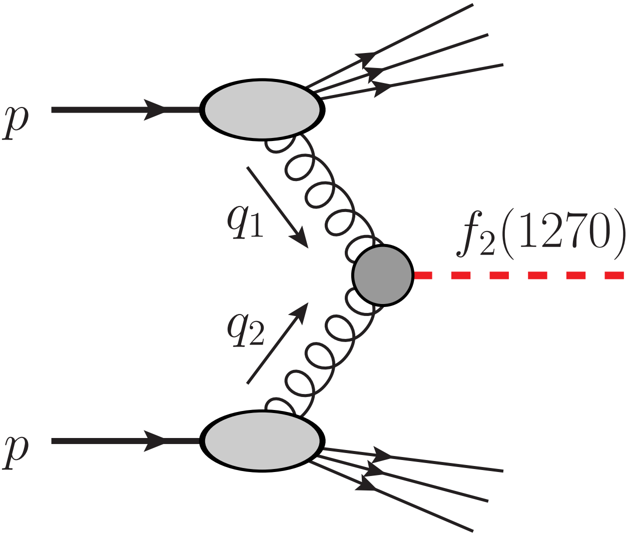

Ewerz-Maniatis-Nachtmann (EMN) vertex

$$\Gamma^{(f_2\gamma\gamma)}_{\mu\nu\kappa\lambda}(q_1,q_2) = 2a_{f_2\gamma\gamma}\,\Gamma^{(0)}_{\mu\nu\kappa\lambda}(q_1,q_2)\,F^{(0)}(Q_1^2,Q_2^2) - b_{f_2\gamma\gamma}\,\Gamma^{(2)}_{\mu\nu\kappa\lambda}(q_1,q_2)\,F^{(2)}(Q_1^2,Q_2^2)\,, \quad (46)$$

with two rank-four tensor functions,

$$\Gamma^{(0)}_{\mu\nu\kappa\lambda}(q_1,q_2) = \left[(q_1\cdot q_2)g_{\mu\nu} - q_{2\mu}q_{1\nu}\right]\left[q_{1\kappa}q_{2\lambda} + q_{2\kappa}q_{1\lambda} - \frac{1}{2}(q_1\cdot q_2)g_{\kappa\lambda}\right], \quad (47)$$

$$\begin{aligned}\Gamma^{(2)}_{\mu\nu\kappa\lambda}(q_1,q_2) = {} & (q_1\cdot q_2)(g_{\mu\kappa}g_{\nu\lambda} + g_{\mu\lambda}g_{\nu\kappa}) + g_{\mu\nu}(q_{1\kappa}q_{2\lambda} + q_{2\kappa}q_{1\lambda}) \\ & - q_{1\nu}q_{2\lambda}g_{\mu\kappa} - q_{1\nu}q_{2\kappa}g_{\mu\lambda} - q_{2\mu}q_{1\lambda}g_{\nu\kappa} - q_{2\mu}q_{1\kappa}g_{\nu\lambda} \\ & - [(q_1\cdot q_2)g_{\mu\nu} - q_{2\mu}q_{1\nu}]\,g_{\kappa\lambda}\,, \quad (48)\end{aligned}$$

Ewerz-Maniatis-Nachtmann (EMN) vertex

To obtain $a_{f_2\gamma\gamma}$ and $b_{f_2\gamma\gamma}$ in (46) we use the values

$$\Gamma(f_2 \to \gamma\gamma) = (2.93 \pm 0.40)\,\mathrm{keV}\,,$$
$$\text{helicity zero contribution} \approx 9\% \text{ of } \Gamma(f_2 \to \gamma\gamma)\,. \quad (49)$$

Using the exp. decay rate

$$\Gamma(f_2 \to \gamma\gamma) = \frac{m_{f_2}}{80\pi}\left(\frac{1}{6}m_{f_2}^6|a_{f_2\gamma\gamma}|^2 + m_{f_2}^2|b_{f_2\gamma\gamma}|^2\right), \quad (50)$$

and assuming $a_{f_2\gamma\gamma} > 0$ and $b_{f_2\gamma\gamma} > 0$, we find

$$a_{f_2\gamma\gamma} = \alpha_{\mathrm{em}} \times 1.17\ \mathrm{GeV}^{-3}\,, \quad (51)$$
$$b_{f_2\gamma\gamma} = \alpha_{\mathrm{em}} \times 2.46\ \mathrm{GeV}^{-1}\,, \quad (52)$$

where $\alpha_{\mathrm{em}} = e^2/(4\pi) \simeq 1/137$ is the electr. coupling constant.

Pascalutsa-Pauk-Vanderhaeghen (PPV) vertex

Poppe and Pascalutsa et al. shown that the most general amplitude for the process $\gamma^*(q_1, \lambda_1) + \gamma^*(q_2, \lambda_2) \rightarrow f_2(\Lambda)$, describing the transition from an initial state of two virtual photons to a tensor meson f_2 ($J^{PC} = 2^{++}$) with mass m_{f_2} and helicity $\Lambda = \pm 2, \pm 1, 0$, involves five independent structures (invariant amplitudes).

Pascalutsa-Pauk-Vanderhaeghen (PPV) vertex

In the formalism presented by Pascalutsa et al. the $\gamma^*\gamma^* \to f_2(1270)$ vertex is parameterized as

$$
\begin{aligned}
\Gamma^{(f_2\gamma\gamma)}_{\mu\nu\kappa\lambda}(q_1, q_2) \quad = \quad & 4\pi\alpha_{\rm em} \Bigg\{ \left[R_{\mu\kappa}(q_1,q_2)R_{\nu\lambda}(q_1,q_2) + \frac{s}{8X} R_{\mu\nu}(q_1,q_2)(q_1-q_2)_\kappa\,(q_1-q_2)_\lambda \right] \\
& \times \frac{\nu}{m_{f_2}} T^{(2)}(Q_1^2, Q_2^2) \\
& + R_{\nu\kappa}(q_1,q_2)(q_1-q_2)_\lambda \left(q_{1\mu} + \frac{Q_1^2}{\nu} q_{2\mu} \right) \frac{1}{m_{f_2}} T^{(1)}(Q_1^2, Q_2^2) \\
& + R_{\mu\kappa}(q_1,q_2)(q_2-q_1)_\lambda \left(q_{2\nu} + \frac{Q_2^2}{\nu} q_{1\nu} \right) \frac{1}{m_{f_2}} T^{(1)}(Q_2^2, Q_1^2) \\
& + R_{\mu\nu}(q_1,q_2)(q_1-q_2)_\kappa\,(q_1-q_2)_\lambda \, \frac{1}{m_{f_2}} T^{(0,T)}(Q_1^2, Q_2^2) \\
& + \left(q_{1\mu} + \frac{Q_1^2}{\nu} q_{2\mu} \right) \left(q_{2\nu} + \frac{Q_2^2}{\nu} q_{1\nu} \right) (q_1-q_2)_\kappa (q_1-q_2)_\lambda \frac{1}{m_{f_2}^3} T^{(0,L)}(Q_1^2, Q_2^2) \Bigg\} ,
\end{aligned}
\tag{53}
$$

Pascalutsa-Pauk-Vanderhaeghen (PPV) vertex

where photons with momenta q_1 and q_2 have virtualities, $Q_1^2 = -q_1^2$ and $Q_2^2 = -q_2^2$, $s = (q_1 + q_2)^2 = 2\nu - Q_1^2 - Q_2^2$, $X = \nu^2 - q_1^2 q_2^2$, $\nu = (q_1 \cdot q_2)$, and

$$R_{\mu\nu}(q_1, q_2) = -g_{\mu\nu} + \frac{1}{X}\left[\nu\left(q_{1\mu}q_{2\nu} + q_{2\mu}q_{1\nu}\right) - q_1^2 q_{2\mu}q_{2\nu} - q_2^2 q_{1\mu}q_{1\nu}\right] \tag{54}$$

$T^{(\Lambda)}(Q_1^2, Q_2^2)$ are the $\gamma^*\gamma^* \to f_2(1270)$ transition form factors for Λ $f_2(1270)$ helicity.For the case of helicity zero, there are two form factors depending on whether both photons are transverse (superscript T) or longitudinal (superscript L). We can express the transition form factors as

$$T^{(\Lambda)}(Q_1^2, Q_2^2) = F^{(\Lambda)}(Q_1^2, Q_2^2)\, T^{(\Lambda)}(0, 0)\,. \tag{55}$$

In the limit $Q_{1,2}^2 \to 0$ only $T^{(0,T)}$ and $T^{(2)}$ contribute.

EMN vs PPV vertices

Comparing the two approaches at both real photons ($Q_1^2 = Q_2^2 = 0$) and at $\sqrt{s} = m_{f_2}$ we found the correspondence

$$4\pi\alpha_{\rm em}\, T^{(0,T)}(0,0) = -a_{f_2\gamma\gamma}\,\frac{m_{f_2}^3}{2}\,, \tag{56}$$

$$4\pi\alpha_{\rm em}\, T^{(2)}(0,0) = -b_{f_2\gamma\gamma}\,2m_{f_2}\,. \tag{57}$$

$g^*g^* \longrightarrow f_2(1270)$ form factor(s)

$f_2(1270)$ is extended, finite size object and one can expect an additional form factor(s) $F(Q_1^2, Q_2^2)$ associated with the gluon virtualities for the $g^*g^* \rightarrow f_2$ vertex. In our work the form factor is parametrized as:

$$F(Q_1^2, Q_2^2) = \frac{\Lambda_M^2}{Q_1^2 + Q_2^2 + \Lambda_M^2}, \quad (58)$$

$$F(Q_1^2, Q_2^2) = \left(\frac{\Lambda_D^2}{Q_1^2 + Q_2^2 + \Lambda_D^2}\right)^2, \quad (59)$$

$$F(Q_1^2, Q_2^2) = \frac{\Lambda_1^2}{Q_1^2 + \Lambda_1^2} \frac{\Lambda_1^2}{Q_2^2 + \Lambda_1^2}, \quad (60)$$

$$F(Q_1^2, Q_2^2) = \frac{\Lambda_2^4}{(Q_1^2 + \Lambda_2^2)^2} \frac{\Lambda_2^4}{(Q_2^2 + \Lambda_2^2)^2}, \quad (61)$$

where Λ is a parameter whose value is expected to be close to the resonance mass.

No form factor in earlier work by Jeon et al.

k_t-factorization approach

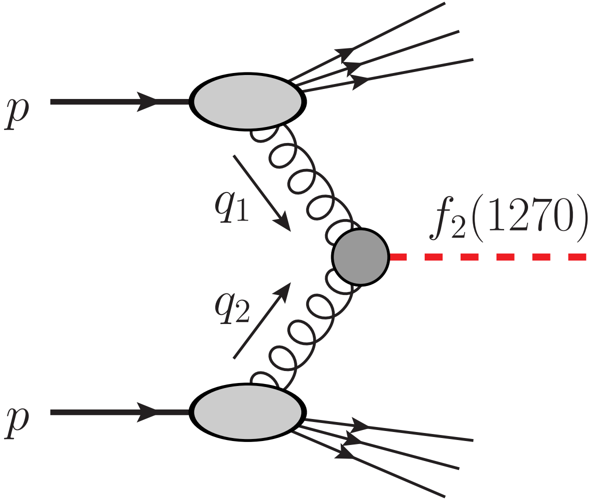

Rysunek: General diagram for inclusive $f_2(1270)$ production via gluon-gluon fusion in proton-proton collisions.

k_t-factorization approach

The differential cross section for inclusive $f_2(1270)$ meson production via the $g^* g^* \to f_2(1270)$ fusion in the k_t-factorization approach can be written as:

$$\frac{d\sigma}{dy d^2\boldsymbol{p}} = \int \frac{d^2\boldsymbol{q}_1}{\pi \boldsymbol{q}_1^2} \mathcal{F}_g(x_1, \boldsymbol{q}_1^2) \int \frac{d^2\boldsymbol{q}_2}{\pi \boldsymbol{q}_2^2} \mathcal{F}_g(x_2, \boldsymbol{q}_2^2)\, \delta^{(2)}(\boldsymbol{q}_1 + \boldsymbol{q}_2 - \boldsymbol{p}) \frac{\pi}{(x_1 x_2 s)^2} \overline{|\mathcal{M}_{g^* g^* \to f_2}|^2}\,. \quad (62)$$

Here $\boldsymbol{q}_1$, $\boldsymbol{q}_2$ and $\boldsymbol{p}$ - the transverse momenta of the gluons and the $f_2(1270)$ meson. The f_2 meson is on-shell and $p^2 = m_{f_2}^2$. $\mathcal{M}_{g^* g^* \to f_2}$ is the off-shell matrix element for the hard subprocess and $\mathcal{F}_g$ are the unintegrated gluon distribution functions (UGDFs). The UGDFs depend on gluon longitudinal momentum fractions $x_{1,2} = m_T \exp(\pm \mathrm{y})/\sqrt{s}$ and $\boldsymbol{q}_1^2, \boldsymbol{q}_2^2$ entering the hard process. In principle, they can depend also on factorization scales $\mu_{F,i}^2$, $i = 1, 2$. We assume $\mu_{F,1}^2 = \mu_{F,2}^2 = m_T^2$. Here m_T is transverse mass of the $f_2(1270)$ meson; $m_T = \sqrt{\boldsymbol{p}^2 + m_{f_2}^2}$. The $\delta^{(2)}$ function above can be eliminated by introducing $\boldsymbol{q}_1 + \boldsymbol{q}_2$ and $\boldsymbol{q}_1 - \boldsymbol{q}_2$

k_t-factorization approach

The off-shell matrix element can be written as (we restore the color-indices a and b)

$$\mathcal{M}^{ab} = \frac{q_{1t}^{\mu} q_{2t}^{\nu}}{|\boldsymbol{q}_1||\boldsymbol{q}_2|} \mathcal{M}_{\mu\nu}^{ab} = \frac{q_{1+} q_{2-}}{|\boldsymbol{q}_1||\boldsymbol{q}_2|} n^{+\mu} n^{-\nu} \mathcal{M}_{\mu\nu}^{ab} = \frac{x_1 x_2 s}{2|\boldsymbol{q}_1||\boldsymbol{q}_2|} n^{+\mu} n^{-\nu} \mathcal{M}_{\mu\nu}^{ab} (6$$

with the lightcone components of gluon momenta $q_{1+} = x_1 \sqrt{s/2}$, $q_{2-} = x_2 \sqrt{s/2}$. Here the matrix-element reads

$$\mathcal{M}_{\mu\nu} = \Gamma_{\mu\nu\kappa\lambda}^{(f_2\gamma\gamma)}(q_{1t}, q_{2t}) \left(\epsilon^{(f_2)\kappa\lambda}(p)\right)^* , \qquad (64)$$

where $\epsilon^{(f_2)}$ is the polarisation tensor for the $f_2(1270)$ meson.

k_t-factorization approach, energy-momentum tensor

In the k_t-factorization approach in Jeon et al. the matrix element squared was written as:

$$\overline{|\mathcal{M}_{g^*g^*\to f_2}|^2} = \frac{1}{4}\sum_{\lambda_1,\lambda_2,\lambda_{f_2}} |\mathcal{M}_{g^*g^*\to f_2}|^2$$

$$= \frac{1}{4}\frac{1}{(N_c^2-1)^2}\sum_{a,b}\frac{q_{1t\,\mu_1}}{q_{1t}}\frac{q_{2t\,\nu_1}}{q_{2t}}V_{ab}^{\alpha_1\beta_1\mu_1\nu_1}(q_1,q_2)\,P^{(2)}_{\alpha_1\beta_1,\alpha_2\beta_2}(p)\frac{q_{1t\,\mu_2}}{q_{1t}}\frac{q_{2t\,\nu_2}}{q_{2t}}\left(V_{ab}^{\alpha_2\beta_2\mu_2\nu_2}(q_1,q_2)\right)^*$$

$$= \frac{1}{4}\frac{1}{(N_c^2-1)\kappa^2}P^{(2)}_{\alpha_1\beta_1,\alpha_2\beta_2}(p)H_\perp^{\alpha_1\beta_1}(q_{1t},q_{2t})H_\perp^{\alpha_2\beta_2}(q_{1t},q_{2t})\left(\frac{x_1x_2s}{2q_{1t}q_{2t}}\right)^2, \quad (65$$

where $\lambda_1, \lambda_2, \lambda_{f_2}$ are the helicities of the gluons and f_2 meson, a, b are color indices, N_c is the number of colors, $V_{ab}^{\alpha\beta\mu\nu}$ is the $gg\to f_2$ vertex. (see Jeon et al.) and $\kappa \approx \mathcal{O}(0.1\,\mathrm{GeV})$ is to be fixed by experiment.
No form factor(s), no α_s.

k_t-factorization approach

The $g^* g^* \to f_2(1270)$ coupling entering in the matrix element squared can be obtained from that for $\gamma^*\gamma^* \to f_2(1270)$ coupling as:

$$\alpha_{\rm em}^2 \to \alpha_{\rm s}^2 \, \frac{1}{4N_c(N_c^2-1)} \, \frac{1}{(< e_q^2 >)^2} \, . \qquad (66)$$

Here $(< e_q^2 >)^2 = 25/162$ for the $\frac{1}{\sqrt{2}}\left(u\bar{u} + d\bar{d}\right)$ flavour structure.

In realistic calculations the running of strong coupling constants must be included. In our numerical calculations presented below the renormalization scale is taken in the form:

$$\alpha_{\rm s}^2 \to \alpha_{\rm s}(\max\{m_T^2, \boldsymbol{q}_1^2\})\, \alpha_{\rm s}(\max\{m_T^2, \boldsymbol{q}_2^2\}) \, . \qquad (67)$$

The Shirkov-Solovtsov prescription is used to extrapolate down to small renormalization scales. The strong coupling constant was not included by Jeon et al.

A simple $\pi\pi$ final-state rescattering model

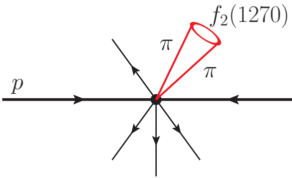

Rysunek: General diagram for the $\pi\pi$ final-state rescattering leading to $f_2(1270)$ production in proton-proton collisions.

Both $\pi^+\pi^-$ and $\pi^0\pi^0$ rescatterings may lead to the production of the $f_2(1270)$ meson.

A simple $\pi\pi$ final-state rescattering model

The spectrum of pions will be not calculated here but instead we will use a Lévy parametrization of the inclusive π^0 cross section for $\sqrt{s} = 7$ TeV. At the ALICE energies and midrapidities we assume the following relation:

$$\frac{d\sigma^{\pi^+}}{d\mathrm{y}dp_t}(\mathrm{y},p_t) = \frac{d\sigma^{\pi^-}}{d\mathrm{y}dp_t}(\mathrm{y},p_t) = \frac{d\sigma^{\pi^0}}{d\mathrm{y}dp_t}(\mathrm{y},p_t) \qquad (68)$$

to be valid.

Our approach here is similar in spirit to color evaporation approach considered, e.g. for J/ψ.

A simple $\pi\pi$ final-state rescattering model

We write the number of produced $f_2(1270)$ per event as

$$N = \int d\mathrm{y}_1 dp_{1t} \int d\mathrm{y}_2 dp_{2t} \int \frac{d\phi_1}{2\pi} \frac{d\phi_2}{2\pi} \frac{dN^\pi}{d\mathrm{y}_1 dp_{1t}} \frac{dN^\pi}{d\mathrm{y}_2 dp_{2t}} P_{\pi\pi\to f_2} , \tag{69}$$

where $dN^\pi/(d\mathrm{y} dp_t)$ is number of pions per interval of rapidity and transverse momentum. Here we use the Tsallis parametrization of π^0 at $\sqrt{s} = 7$ TeV (Abelev et al.). Above $P_{\pi\pi\to f_2}$ parametrizes probability of the $\pi^+\pi^-$ and $\pi^0\pi^0$ formation of $f_2(1270)$ as well as probability of its survival in a dense hadronic system. It will be treated here as a free parameter adjusted to the $f_2(1270)$ data from the Lee thesis. The distribution $dN^\pi/(d\mathrm{y} dp_t)$ is obtained then by calculating y and p_t of the $f_2(1270)$ meson and binning in these variables. The effect of hadronic rescattering is also discussed recently by Utheim and Sjöstrand.

Numerical Results

To convert to the number of $f_2(1270)$ mesons per event (ALICE data) we use the following relation:

$$\frac{dN}{dp_t} = \frac{1}{\sigma_{\rm inel}} \frac{d\sigma}{dp_t} \,. \qquad (70)$$

The inelastic cross section for $\sqrt{s} = 7$ TeV was measured at the LHC and is:

$$\sigma_{\rm inel} = 73.15 \pm 1.26\,({\rm syst.})\,{\rm mb}\,, \qquad (71)$$

$$\sigma_{\rm inel} = 71.34 \pm 0.36\,({\rm stat.}) \pm 0.83\,({\rm syst.})\,{\rm mb}\,, \qquad (72)$$

as obtained by the TOTEM (Antchev et al.) and ATLAS (Aad et al.) collaborations, respectively. We take $\sigma_{\rm inel} = 72.5$ mb.

Numerical Results

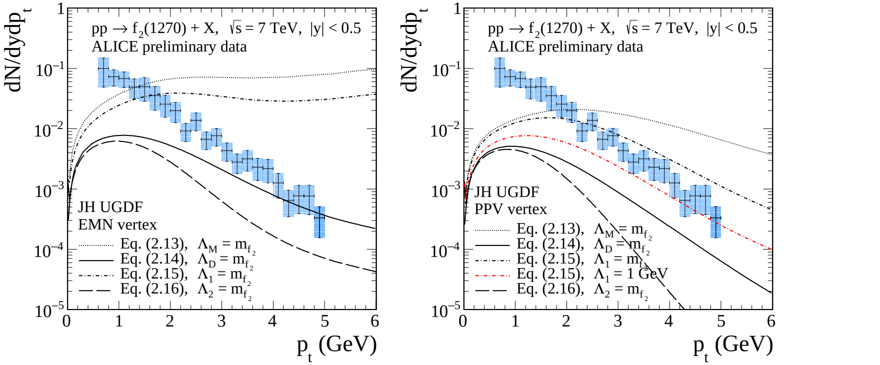

Rysunek: The $f_2(1270)$ meson transverse momentum distributions at $\sqrt{s} = 7$ TeV and $|\mathrm{y}| < 0.5$. The preliminary ALICE data from Lee thesis. The results for the EMN (left panel) and PPV (right panel) $g^*g^* \to f_2(1270)$ vertex for different $F(Q_1^2, Q_2^2)$ ff are shown. In this calculation the JH UGDF was used.

Numerical Results

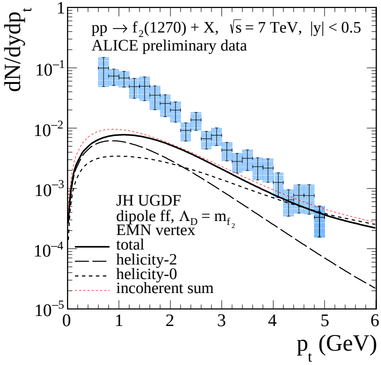

Rysunek: The $f_2(1270)$ meson transverse momentum distributions at $\sqrt{s} = 7$ TeV and $|\mathrm{y}| < 0.5$ together with the preliminary ALICE data. Shown are the results calculated in the two approaches, EMN (left panel) and PPV (right panel) vertices, and the helicity-0 and -2 components separately and their coherent sum (total). Here we used dipole form factor parametrization with $\Lambda_D = m_{f_2}$. The dotted line corresponds to the contribution for the

Numerical Results

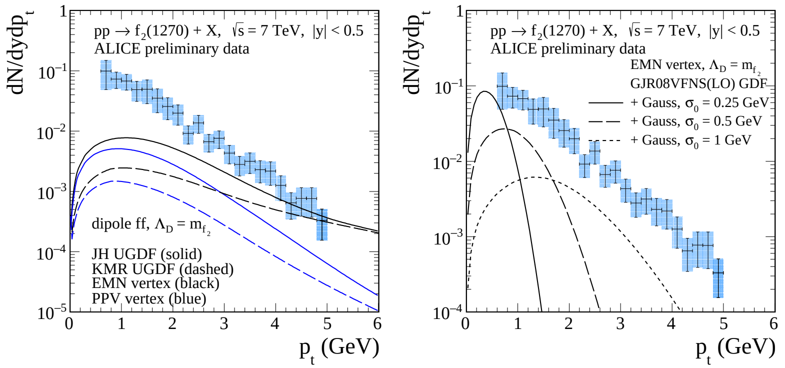

Rysunek: The $f_2(1270)$ meson transverse momentum distributions at $\sqrt{s} = 7$ TeV and $|\mathrm{y}| < 0.5$ together with the preliminary ALICE data from the Lee thesis. In the left panel two different UGDFs, JH (solid lines) and KMR (dashed lines), are shown. In the right panels the dependence on the Gaussian smearing parameter σ_0 for GJR08VFNS(LO) GDF. Here the EMN vertex and the dipole form factor with $\Lambda_D = m_{f_2}$ were used.

Numerical Results

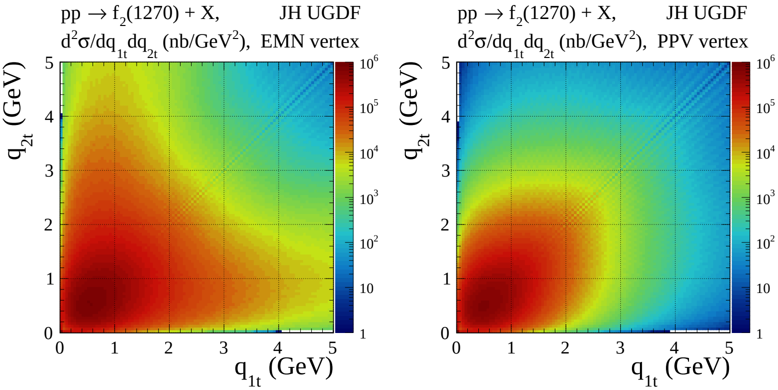

Rysunek: Two-dimensional distributions in gluon transverse momenta for the JH UGDF and for two $g^* g^* f_2(1270)$ vertex prescription: EMN (left panel) and PPV (right panel). Here we used the dipole form factor with $\Lambda_D = m_{f_2}$.

Numerical Results

We have checked that

$$\frac{d^2\sigma_{\rm EMN}}{dq_{1t}dq_{2t}}\left(\frac{d^2\sigma_{\rm PPV}}{dq_{1t}dq_{2t}}\right)^{-1} \to 1\,, \quad \text{for} \;\; q_{1t}\to 0 \;\; \text{and} \;\; q_{2t}\to 0\,, \tag{73}$$

i.e. the two vertices are equivalent for both on-shell photons.

Numerical Results

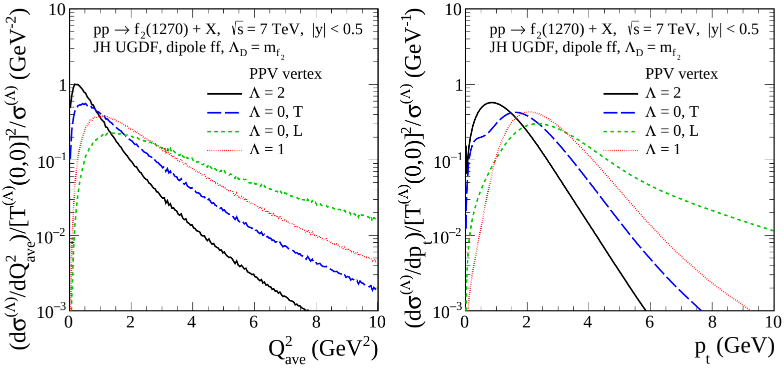

Rysunek: Normalized distributions in averaged virtuality $Q^2_{\rm ave} = (Q_1^2 + Q_2^2)/2$ (left panel) and in the $f_2(1270)$ meson transverse momentum (right panel). Results for different $\Lambda = 0, 1, 2$ terms in the $g^* g^* f_2$ vertex using the same form of $F^{(\Lambda)}(Q_1^2, Q_2^2)$ with $\Lambda_D = m_{f_2}$ are shown. JH UGDF was used.

Numerical Results

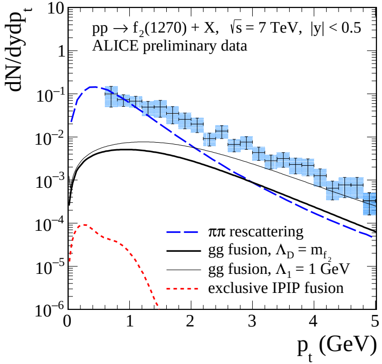

Rysunek: Results for the $\pi\pi$ rescattering mechanism (long-dashed line), for the gg-fusion mechanism (solid lines), and for the $\mathbb{P}\mathbb{P}$ fusion mechanism (dotted line) together with the preliminary ALICE data. We show maximal allowed contribution from the $\pi\pi$ rescattering. The results for gg-fusion contributions were calculated for JH UGDF and for the PPV vertex [only helicity-2 and helicity (0, T) terms] and for two form factor functions (top

Comment on exclusive $pp \to pp f_2(1270)$ process

We present the Born result (without absorptive corrections important only when restricting to purely exclusive processes) for the $pp \to pp f_2(1270)$ process proceeding via the pomeron-pomeron fusion mechanism calculated in the tensor-pomeron approach.
In the calculation we take the $\mathbb{P} - \mathbb{P} - f_2(1270)$ coupling parameters from Lebiedowicz-Nachtmann-Szczurek 2018.

Inclusive ϕ production

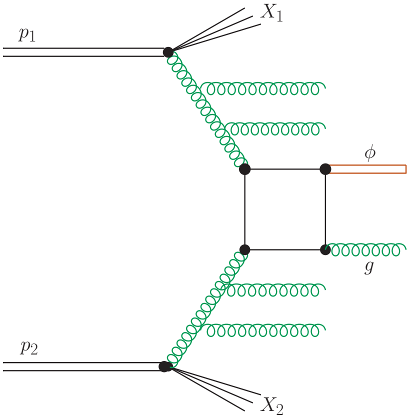

Rysunek: The leading-order diagram for direct ϕ meson production in the k_t-factorization approach.

spin-1, C $= +1$ as for inclusive J/ψ

Inclusive ϕ production

We calculate the dominant color-singlet $gg \to \phi g$ contribution. In the k_t-factorization the NLO differential cross section can be written as:

$$\frac{d\sigma(pp \to \phi g X)}{dy_{J/\psi} dy_g d^2 p_{\phi,t} d^2 p_{g,t}} = \frac{1}{16\pi^2 \hat{s}^2} \int \frac{d^2 q_{1t}}{\pi} \frac{d^2 q_{2t}}{\pi} \overline{|\mathcal{M}^{off-shell}_{g^* g^* \to \phi g}|^2} \times \delta^2 \left(\vec{q}_{1t} + \vec{q}_{2t} - \vec{p}_{H,t} - \vec{p}_{g,t} \right) \mathcal{F}_g(x_1, q_{1t}^2, \mu^2) \mathcal{F}_g(x_2, q_{2t}^2, \mu^2) \quad (74)$$

where $\mathcal{F}_g$ are unintegrated gluon distributions. The matrix elements were calculated as done e.g. for $J/\psi g$ production. The corresponding matrix element squared for the $gg \to \phi g$ is

$$|\mathcal{M}_{gg \to \phi g}|^2 \propto \alpha_s^3 |R(0)|^2 \, . \quad (75)$$

Inclusive ϕ production

Running coupling contants are used in the calculation.
Different combination of renormalization scales were tried.
Finally we decided to use:

$$\alpha_s^3 \to \alpha_s(\mu_1^2)\alpha_s(\mu_2^2)\alpha_s(\mu_3^2) \;, \tag{76}$$

where $\mu_1^2 = \max(q_{1t}^2, m_t^2)$, $\mu_2^2 = \max(q_{2t}^2, m_t^2)$ and $\mu_3^2 = m_t^2$, where here m_t is the ϕ transverse mass. The factorization scale in the calculation was taken as $\mu_F^2 = (m_t^2 + p_{t,g}^2)/2$. The radial wave function at zero can be estimated from the decay of $\phi \to l^+l^-$ as is usually done for $J/\psi(c\bar{c})$, see e.g. Mangoni et al.

$$\Gamma(\phi \to l^+l^-) = 16\pi \frac{\alpha Q_s^2}{M_\phi^2} |\Psi_\phi(0)|^2 \left(1 - \frac{16}{3}\frac{\alpha_s}{\pi}\right) \;, \tag{77}$$

where Q_s is fractional charge of the s quark. Then

$$|\Psi_\phi(0)|^2 = \frac{\Gamma(\phi \to l^+l^-)}{16\pi\alpha_{em}Q_s^2} \frac{M_\phi^2}{1 - 16\alpha_s/(3\pi)} \;. \tag{78}$$

Inclusive ϕ production, results

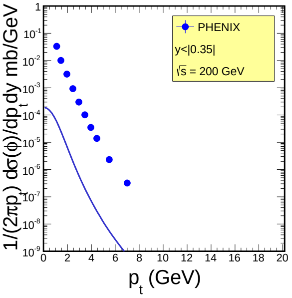

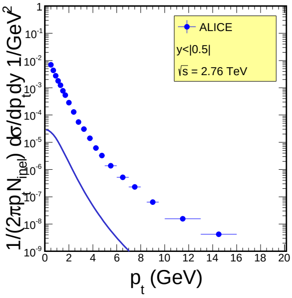

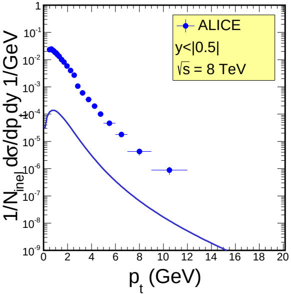

Inclusive ϕ production, results

For each considered case the result of calculation is below the experimental data.
This suggests that the gluon-gluon fusion is not the dominant production mechanism of ϕ meson production.
The fragmentation mechanism was considered in the literature and it may be the dominant mechanism of ϕ meson production.

Inclusive η' production

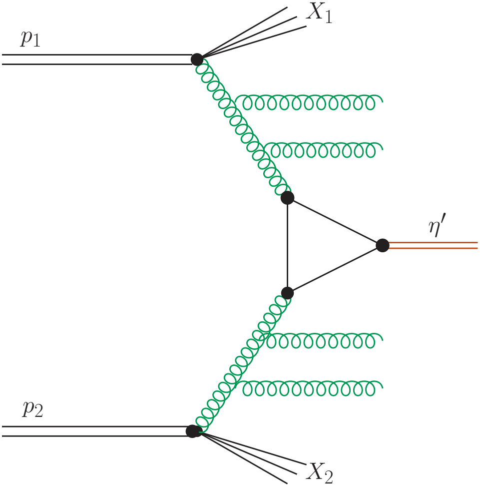

Rysunek: The leading-order diagram for η' meson production in the k_t-factorization approach.

Inclusive η' production

Here the lowest-order subprocess $gg \to \eta'$ is allowed by positive C-parity of η' mesons. In the k_t-factorization approach the leading-order cross section for the η' meson production can be written as:

$$\sigma_{pp\to\eta'} = \int dy d^2p_t d^2q_t \frac{1}{sx_1x_2} \frac{1}{m^2_{t,\eta'}} \overline{|\mathcal{M}_{g^*g^*\to\eta'}|^2} \mathcal{F}_g(x_1, q^2_{1t}, \mu^2_F) \mathcal{F}_g(x_2, q^2_{2t}, \mu^2_F)/4 \,, \quad (79)$$

Above $\mathcal{F}_g$ are unintegrated gluon distributions and $\mathcal{M}_{g^*g^*\to\eta'}$ is $g^*g^* \to \eta'$ (off-shell) matrix element. In the last equation: $\vec{p}_t = \vec{q}_{1t} + \vec{q}_{2t}$ is transverse momentum of the η' meson and $\vec{q}_t = \vec{q}_{1t} - \vec{q}_{2t}$ is auxiliary variable which is used in the integration.

Inclusive η' production

Furthermore: $m_{t,\eta'}$ is the so-called η' transverse mass and $x_1 = \frac{m_{t,\eta'}}{\sqrt{s}} \exp(y)$, $x_2 = \frac{m_{t,\eta'}}{\sqrt{s}} \exp(-y)$. The factor $\frac{1}{4}$ is the jacobian of transformation from $(\vec{q}_{1t}, \vec{q}_{2t})$ to $(\vec{p}_t, \vec{q}_t)$ variables.
As for ϕ production the running coupling contants are used. Different combination of scales are tried. The best choice is:

$$\alpha_s^2 \to \alpha_s(\mu_1^2)\alpha_s(\mu_2^2) \; , \tag{80}$$

where $\mu_1^2 = \max(q_{1t}^2, m_t^2)$ and $\mu_2^2 = \max(q_{2t}^2, m_t^2)$. Above m_t is transverse mass of the η' meson. The factorization scale(s) for the η' meson production are fixed traditionally as $\mu_F^2 = m_t^2$.
The $g^*g^* \to \eta'$ coupling has relatively simple one-term form:

$$T_{\mu\nu}(q_1, q_2) = F_{g^*g^*\to\eta'}(q_1, q_2)\epsilon_{\mu\nu\alpha\beta} q_1^\alpha q_2^\beta \; , \tag{81}$$

where $F_{g^*g^*\to\eta'}(q_1, q_2)$ object is known as the two-gluon transition form factor.

Inclusive η' production

The matrix element to be used in the k_t-factorization is then:

$$\mathcal{M}^{ab} = \frac{q^{\mu}_{1,\perp} q^{\nu}_{2,\perp}}{|\mathbf{q}_1||\mathbf{q}_2|} T_{\mu\nu} \; . \tag{82}$$

In contrast to the convention for two-photon transition form factor the strong coupling constants are usually absorbed into the two-gluon form factor definition.
The matrix element squared for the $gg \to \eta'$ subprocess is

$$|\mathcal{M}_{gg\to\eta'}|^2 \propto F^2_{g^*g^*\to\eta'}(q^2_{1t}.q^2_{2t}) \propto \alpha_s^2 F^2_{\gamma^*\gamma^*\to\eta'}(q^2_{1t}.q^2_{2t}) \; , \tag{83}$$

where $F^2_{g^*g^*\to\eta'}(q^2_{1t}, q^2_{2t})$ and $F^2_{\gamma^*\gamma^*\to\eta'}(q^2_{1t}, q^2_{2t})$ are two-gluon and two-photon transition form factors of the η' meson, respectively.

Inclusive η' production

It was discussed by Kroll-Passek-Kumericki, in leading-twist collinear approximation. Such an approach is valid for $Q_1^2 = q_{1t}^2 \gg 0$ and $Q_2^2 = q_{2t}^2 \gg 0$. Here we need such a transition form factor also for $Q_1^2, Q_1^2 \sim 0$. There is a simple relation between the two-gluon and two-photon form factors for the quark-antiquark systems η' meson may have also the two-gluon component in its Fock decomposition The form factor found there can be approximately parametrized as

$$\bar{Q}^2 F^2_{g^* g^* \to \eta'}(Q_1^2, Q_2^2) \approx 0.2 \pm 0.1 \ \mathrm{GeV} \ , \tag{84}$$

where $\bar{Q}^2 = (Q_1^2 + Q_2^2)/2$. A better approach would be to use their Eqs.(5.13-5.16) with parameters given there. The result from Kroll and Passek-Kumericki is:

$$F(\bar{Q}^2, \omega) = 4\pi\alpha_s \frac{f_P}{\bar{Q}^2} \frac{\sqrt{n_f}}{N_c} A(\omega) \ . \tag{85}$$

Inclusive η' production

In the factorized (in $\bar{Q}^2$ and ω) formula:

$$A(\omega) = A_{q\bar{q}}(\omega) + \frac{N_c}{2n_f} A_{gg}(\omega) \ , \tag{86}$$

where

$$A_{q\bar{q}}(\omega) = \int_0^1 dx \ \Phi_1(x, \mu_F^2) \frac{1}{1 - \omega^2(1-2x)^2} \ , \tag{87}$$

$$A_{gg}(\omega) = \int_0^1 dx \ \frac{\Phi_g(x, \mu_F^2)}{x\bar{x}} \frac{1-2x}{1 - \omega^2(1-2x)^2} \tag{88}$$

and Φ_1 and Φ_g are singlet and gluon distribution functions, respectively. Above

$$\omega = \frac{Q_1^2 - Q_2^2}{Q_1^2 + Q_2^2} \ . \tag{89}$$

Φ_1 and Φ_g undergo QCD evolution (Kroll-Passek-Kumericki) which is included also in the present analysis.

$F_{\gamma^*\gamma^* \to \eta'}$ form factor

In Babiarz et al. we have shown how to calculate the transition form factor from the light-cone $Q\bar{Q}$ wave function of the η_c quarkonium. Here we shall follow the same idea but for light quark and light antiquark system. The flavour wave function of η' meson can be approximated as

$$|\eta'\rangle \approx \frac{1}{\sqrt{3}}(u\bar{u} + d\bar{d} + s\bar{s}) \ . \tag{90}$$

The spatial wave function could be calculated e.g. in potential models. The momentum wave function can be then obtained as a Fourier transform of the spatial one. We shall not follow this path in the present study. Instead we shall take a simple, but reasonable, parametrization of the light-cone wave function. In principle, each component in (90) may have different spatial as well as momentum wave function. Here for simplicity we shall assume one effective wave function for each flavour component. We shall take the simple parametrization

$F_{\gamma^*\gamma^*\to\eta'}$ form factor

The light cone wave function is obtained then via the Terentev's transformation We shall use the normalization of the light cone wave function as:

$$\int_0^1 \frac{dz}{z(1-z)} \frac{d^2k}{16\pi^3} |\phi(z,k_t)|^2 = 1 \,. \tag{92}$$

Above

$$\phi(z,k_t) \propto \sqrt{M_{q\bar{q}}} \exp\left(-p^2/(2\beta^2)\right) \tag{93}$$

and the so-called Terentev's prescription, relating the rest-frame and light-cone variables, is used:

$$p^2 = \frac{1}{4}\left(M_{q\bar{q}}^2 - 4m_{eff}^2\right) \,. \tag{94}$$

Above $M_{q\bar{q}}$ is the invariant mass of the $q\bar{q}$ system. The parameters in the above equations: m_{eff} (hidden in $\phi(z,k_t)$) and β are in principle free. Here we shall take:

$$m_{eff} = (2/3)m_q + (1/3)m_s \,, \tag{95}$$

$F_{\gamma^*\gamma^*\to\eta'}$ form factor

Having fixed light-cone wave function one can calculate electromagnetic $\gamma^*\gamma^* \to \eta'$ transition form factor as:

$$F(Q_1^2, Q_2^2) = -\frac{1}{\sqrt{3}}(e_u^2 + e_d^2 + e_s^2)\sqrt{N_c}\, 4m_{eff} \cdot \int \frac{dz d^2\boldsymbol{k}}{z(1-z)16\pi^3}\psi(z,\boldsymbol{k}) \left\{ \frac{1-z}{(\boldsymbol{k}-(1-z)\boldsymbol{q}_2)^2 + z(1-z)\boldsymbol{q}_1^2 + m_{eff}^2} + \frac{z}{(\boldsymbol{k}+z\boldsymbol{q}_2)^2 + z(1-z)\boldsymbol{q}_1^2 + m_{eff}^2} \right\} \quad (96)$$

The $F(0,0)$ is known and can be calculated from the radiative decay width (BABAR2018).

In the collinear approximation, i.e. when neglecting transverse momenta of photons, also of quark and antiquark in the meson wave function the formula above can be reduced to a single integral

$$F(Q_1^2, Q_2^2) = \frac{1}{\sqrt{3}}(e_u^2 + e_d^2 + e_s^2) f_{\eta'} \cdot \int_0^1 dz \left\{ \frac{(1-z)\phi(z)}{(1-z)^2 Q_1^2 + z(1-z)Q_2^2 + m_{eff}^2} + \frac{z\phi(z)}{z^2 Q_1^2 + z(1-z)Q_2^2 + m_{eff}^2} \right\} \quad (97)$$

where the so-called distribution amplitudes $\phi(z) \propto \int d^2k \Psi(z,\mathbf{k})$ and so-called decay constant $f_{\eta'}$.

$F_{\gamma^*\gamma^*\to\eta'}$ form factor

We shall use also a simple parametrization of the transition form factor called non-factorized monopole for brevity

$$F^{nf,monopole}(Q_1^2, Q_2^2) = F(0,0)\frac{\Lambda^2}{\Lambda^2 + Q_1^2 + Q_2^2} \ . \tag{98}$$

This two-parameter formula can be correctly normalized at $Q_1^2 = 0$ and $Q_2^2 = 0$ (BABAR2018). It has also correct asymptotic dependence on $\bar{Q}^2 = (Q_1^2 + Q_2^2)/2$. This is very similar to the approach done long ago by Brodsky and Lepage in the case of neutral pion.

The so-called vector meson dominance model (factorized monopole)

$$F^{VDM}(Q_1^2, Q_2^2) = F(0,0)\frac{m_V^2}{m_V^2 + Q_1^2}\frac{m_V^2}{m_V^2 + Q_2^2} \tag{99}$$

$F_{g^*g^*\to\eta'}$ form factor

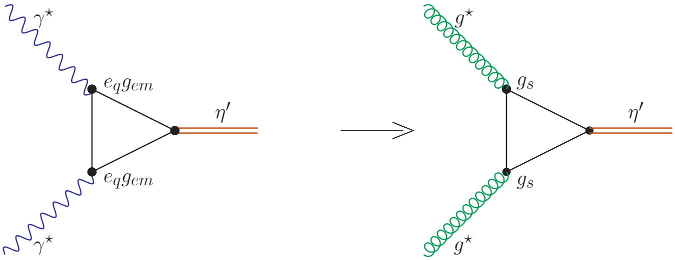

Rysunek: The assumed mechanisms of the $\gamma^*\gamma^* \to \eta'$ (left) and $g^*g^* \to \eta'$ (right) couplings.

$F_{g^* g^* \to \eta'}$ form factor

The two-gluon transition form factor is closely related to two-photon transition form factor provided the meson is of the quark-antiquark type. Then replacing virtual photons by virtual gluons, the electromagnetic coupling constants by the strong coupling constants, correcting by fractional charges of quarks in the electromagnetic case and by color factors being consistent with the unintegrated gluon distributions:

$$|F_{g^* g^* \to \eta'}(Q_1^2, Q_2^2)|^2 = |F_{\gamma^* \gamma^* \to \eta'}(Q_1^2, Q_2^2)|^2 \frac{g_s^2}{g_{em}^2} \frac{1}{4N_c(N_c^2 - 1)} \frac{1}{(< e_q^2 >)^2} \ . \quad (100)$$

Above g_{em}^2 must be taken provided it is included in the definition of $F_{\gamma^* \gamma^* \to \eta'}$ transition form factor. Usually it is not. The relation (100) assumes simplified structure of the meson (η' in our case). Assuming such a relation for η_c meson leads to a fairly good agreement of the transverse momentum distribution of η_c produced in proton-proton collisions with the LHCb data (Babiarz et al.).

Distribution amplitudes from Kroll and Passek-Kumericki

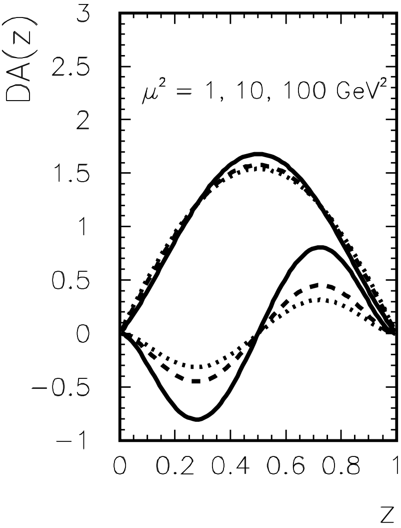

$F_{\gamma^*\gamma^*\to\eta'}$ form factor

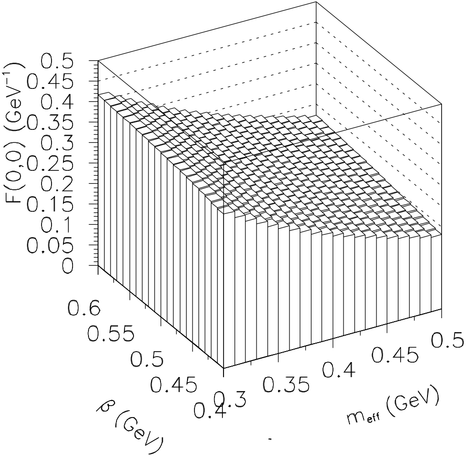

Rysunek: $F_{\gamma^*\gamma^*\to\eta'}(0,0)$ as a function of β and m_{eff}.

$F_{\gamma^*\gamma^*\to\eta'}$ form factor

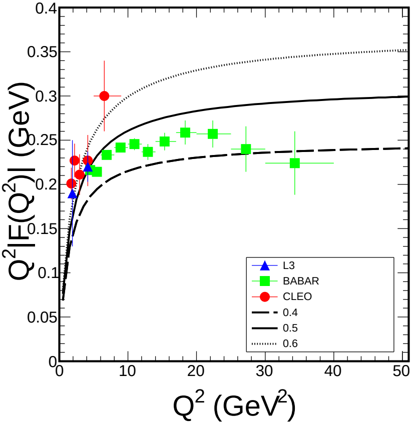

Rysunek: $Q^2F(Q^2)$ as a function of one photon virtuality. We show results for $m_{eff} = 0.4$ GeV and for different values of $\beta = 0.4$, 0.5, 0.6 GeV (from bottom to top). For comparison we show experimental data from CLEO, L3, BABAR.

$F_{\gamma^*\gamma^*\to\eta'}$ form factor

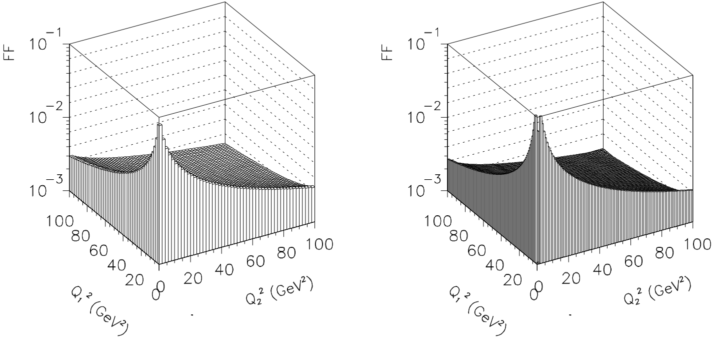

Rysunek: $F_{\gamma^*\gamma^*\to\eta'}(Q_1^2, Q_2^2)$ obtained with the light-cone wave function for $m_{eff} = 0.4$ GeV and $\beta = 0.5$ GeV (left panel) and the leading-twist result (Kroll-Passek-Kumericki) (right panel).

$F_{\gamma^*\gamma^*\to\eta'}$ form factor

In order to better visualize our result we will show also the ratio:

$$R(Q_1^2, Q_2^2) = F^{LC}(Q_1^2, Q_2^2)/F^{nf,monopole}(Q_1^2, Q_2^2) \qquad (102)$$

$F_{\gamma^*\gamma^*\to\eta'}$ form factor

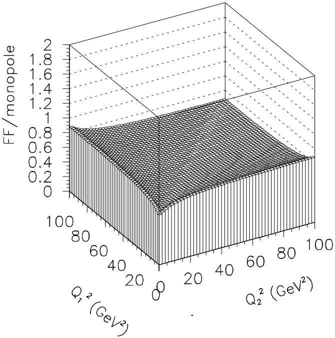

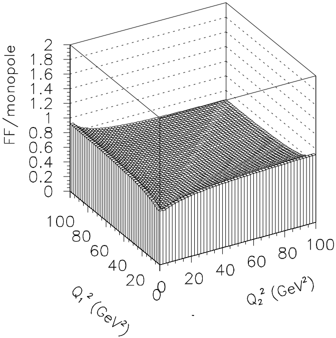

Rysunek: $R(Q_1^2, Q_2^2)$ (see Eq.(102)) with the $\gamma^*\gamma^* \to \eta'$ form factor calculated with η' light-cone wave function (left panel). In this calculation $m_{eff} = 0.4$ GeV and $\beta = 0.5$ GeV is used for example. In the right panel we show similar ratio obtained from Eq.(97) with asymptotic distribution amplitude.

$F_{\gamma^*\gamma^*\to\eta'}$ form factor

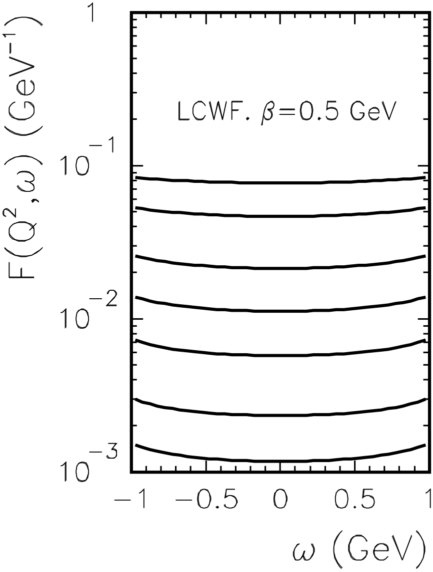

η' production

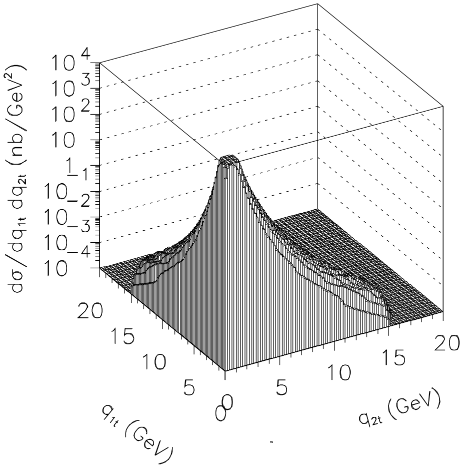

Rysunek: Two-dimensional map in (q_{1t}, q_{2t}) for the full range of η' transverse momentum. Here $\sqrt{s} = 200$ GeV and the KMR UGDF

η' production

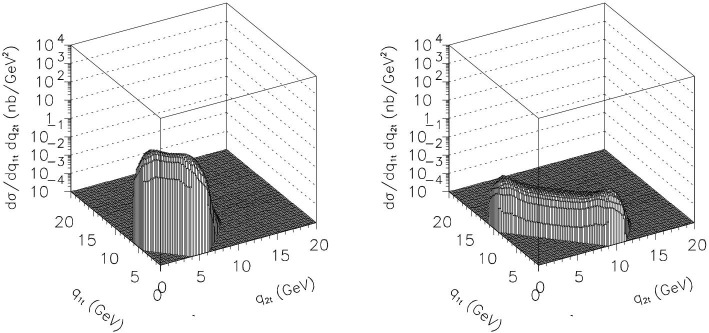

Rysunek: Two-dimensional map in (q_{1t}, q_{2t}) for two different ranges of η' transverse momentum:
4 GeV $< p_t <$ 6 GeV (left panel) and 9 GeV $< p_t <$ 11 GeV (right panel).
Here $\sqrt{s} = 200$ GeV and the KMR UGDF was used.

η' production

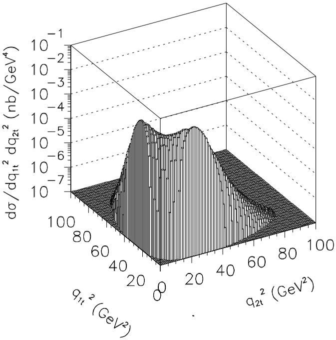

Rysunek: Two-dimensional map in (q_{1t}^2, q_{2t}^2) for 4.5 GeV $< p_t <$ 5.5 GeV (left panel) and 9.5 GeV $< p_t <$ 10.5 GeV (right panel). Here $\sqrt{s}$ = 200 GeV. In this caluculation the KMR UGDF was used and the light-cone wave function with β = 0.5 GeV.

η' production

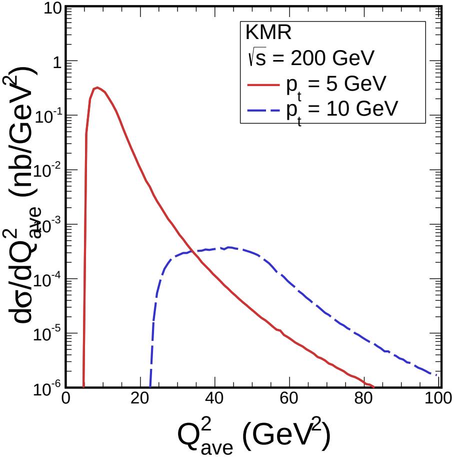

Rysunek: Distribution in $Q^2_{ave} = \bar{Q}^2$ for the two distinct cases:
$p_t = 5 \pm 0.5$ GeV (solid line) and
$p_t = 10 \pm 0.5$ GeV (dashed line).

η' production

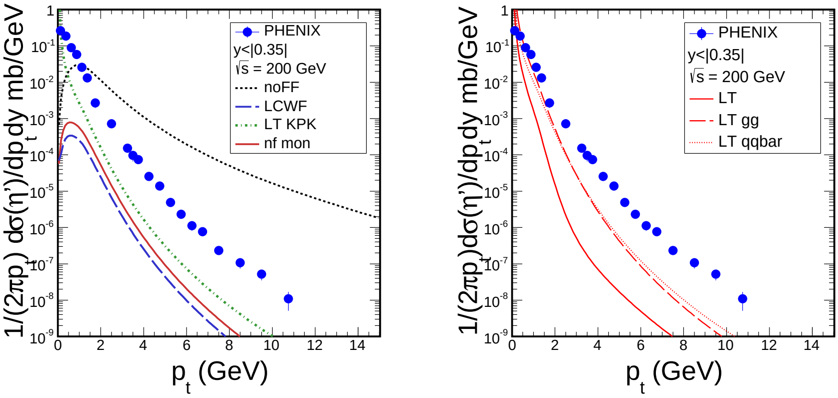

Rysunek: Invariant cross section as a function of meson transverse momentum. Here $\sqrt{s} = 200$ GeV and the KMR UGDF was used in the calculation. In the left panel results for the nonfactorized monopole, LCWF with $\beta = 0.5$ GeV, and simple LT

η' production

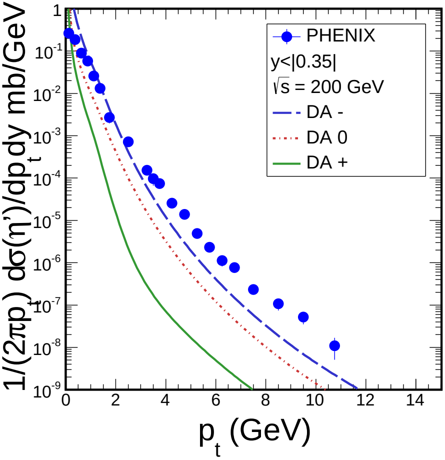

Rysunek: Invariant cross section as a function of meson transverse momentum in the approach with distribution amplitudes and different initial Φ_{gg}. Here $\sqrt{s} = 200$ GeV and the KMR UGDF was

η' production

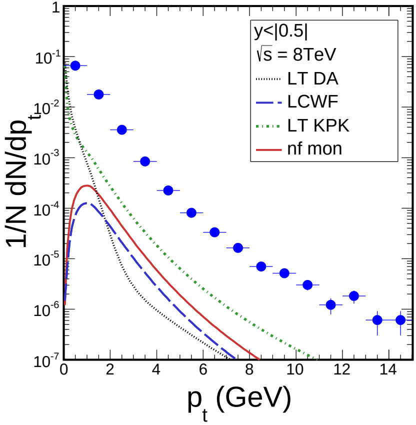

Rysunek: Number of η' mesons per event as a function of meson transverse momentum. Here $\sqrt{s} = 8$ TeV and the KMR UGDF was used in the calculation. The result of the Lund string model simulations is shown as "data points" for comparison.

Conclusions

- Production of several isoscalar mesons is not well understood.
- The gluon-gluon fusion has been discussed as a potentially important mechanism.
- It seems dominant mechanism for pseudoscalar quarkonia, such as η_c.
  It almost fully explains the LHCb experimental data.
- For $f_0(980)$ and $f_2(1270)$ it is probably sizeable mechanism but cannot explain experimental data, especially at low transverse momenta.
- There a coalescence (color evaporation) or FSI pion-pion rescattering models may be alternative solutions.

Conclusions

- In analogy to J/ψ production we have considered $g^*g^* \to \phi g$ partonic process as potential mechanism of the $C = +1$ meson production. The first calulation suggests another mechanism. Parton fragmentation is a candidate.
- We have considered also η' meson production via gluon-gluon fusion. Different explicit approaches to modelling of the $g^*g^* \to \eta'$ coupling have been discussed. The gluon-gluon component in the wave fuction of η' may play a role. The data from LHC would be very useful.
- Combining different mechanisms, including gluon-gluon fusion, may be necessary in future. May be a difficult task.